Härdle, Wolfgang Karl; López Cabrera, Brenda; Okhrin, Ostap; Wang, Weining

**Working Paper**

# Localising temperature risk

SFB 649 Discussion Paper, No. 2011-001

**Provided in Cooperation with:**
Collaborative Research Center 649: Economic Risk, Humboldt University Berlin

*Suggested Citation:* Härdle, Wolfgang Karl; López Cabrera, Brenda; Okhrin, Ostap; Wang, Weining (2010) : Localising temperature risk, SFB 649 Discussion Paper, No. 2011-001, Humboldt University of Berlin, Collaborative Research Center 649 - Economic Risk, Berlin

This Version is available at:
https://hdl.handle.net/10419/56665

SFB 649 Discussion Paper 2011-001

# Localising temperature risk

Wolfgang Karl Härdle*
Brenda López Cabrera*
Ostap Okhrin*
Weining Wang*

* Humboldt-Universität zu Berlin, Germany

This research was supported by the Deutsche Forschungsgemeinschaft through the SFB 649 "Economic Risk".

http://sfb649.wiwi.hu-berlin.de
ISSN 1860-5664

SFB 649, Humboldt-Universität zu Berlin
Spandauer Straße 1, D-10178 Berlin

# Localising temperature risk *

Wolfgang Karl Härdle† Brenda López Cabrera‡ Ostap Okhrin § Weining Wang¶

December 6, 2010

**Abstract**

On the temperature derivative market, modeling temperature volatility is an important issue for pricing and hedging. In order to apply pricing tools of financial mathematics, one needs to isolate a Gaussian risk factor. A conventional model for temperature dynamics is a stochastic model with seasonality and inter temporal autocorrelation. Empirical work based on seasonality and autocorrelation correction reveals that the obtained residuals are heteroscedastic with a periodic pattern. The object of this research is to estimate this heteroscedastic function so that after scale normalisation a pure standardised Gaussian variable appears. Earlier work investigated this temperature risk in different locations and showed that neither parametric component functions nor a local linear smoother with constant smoothing parameter are flexible enough to generally describe the volatility process well. Therefore, we consider a local adaptive modeling approach to find at each time point, an optimal smoothing parameter to locally estimate the seasonality and volatility. Our approach provides a more flexible and accurate fitting procedure of localised temperature risk process by achieving excellent normal risk factors.

Keywords: Weather derivatives, localising temperature residuals, seasonality, local model selection
JEL classification: G19, G29, G22, N23, N53, Q59

*The financial support from the Deutsche Forschungsgemeinschaft via SFB 649 "Ökonomisches Risiko", Humboldt-Universität zu Berlin is gratefully acknowledged.

†Professor at Humboldt-Universität zu Berlin and Director of C.A.S.E. - Center for Applied Statistics and Economics, Humboldt-Universität zu Berlin, Spandauer Straße 1, 10178 Berlin, Germany and National Central University, Graduate Institute for Statistics, No. 300, Jhongda Rd., Jhongli City, Taoyuan County 32001, Taiwan (R.O.C.). Email:haerdle@wiwi.hu-berlin.de

‡Research associate at the Institute for Statistics and Econometrics of Humboldt-Universität zu Berlin, Spandauer Straße 1, 10178 Berlin, Germany. Email:lopezcab@wiwi.hu-berlin.de

§Assistant Professor at the Institute for Statistics and Econometrics of Humboldt-Universität zu Berlin, Spandauer Straße 1, 10178 Berlin, Germany. Email:ostap.okhrin@wiwi.hu-berlin.de

¶Research associate at the Institute for Statistics and Econometrics of Humboldt-Universität zu Berlin, Spandauer Straße 1, 10178 Berlin, Germany. Email:wangwein@cms.hu-berlin.de

# 1 Introduction

Pricing of contingent claims based on stochastic dynamics for example stocks or FX rates is well known in financial engineering. An elegant access of such a pricing task is based on self-financing replication arguments. An essential element of this approach is the tradability of the underlying. This however does not apply to weather derivatives contingent on temperature or rain since the underlying is not tradable. In this context, the proposed pricing techniques are based on either equilibrium ideas (Horst and Mueller (2007)) or econometric modelling of the underlying dynamics (Campbell and Diebold (2005) and Benth, Benth and Koekebakker (2007)) followed by risk neutral pricing.

The equilibrium approach relies on assumptions about preferences (with explicitly known functional forms) though. In this study we prefer a phenomenological approach since the underlying (temperature) we consider is of local nature and our analysis aims at understanding the pricing at different locations and different time points around the world. Such a time series approach has been taken by Benth et al. (2007), who corrects for seasonality (in mean), then for intertemporal correlation and finally as in Campbell and Diebold (2005), for seasonal variation in volatility. After these manipulations a Gaussian risk factor needs to be isolated in order to apply continuous time pricing techniques, Karatzas and Shreve (2001).

Empirical studies following this econometrical route show evidence that the resulting risk factor deviates severely from Gaussianity, which in turn challenges the pricing tools, Benth, Härdle and López Cabrera (2011). In particular, for Asian cities, like for example Kaohsiung (Taiwan), one observes very distinctive non-normality in the form of clearly visible heavy tails caused by extended volatility in peak seasons. This is visible from Figure 1 where a log density plot reveals a nonnormal shoulder structure (kurtosis= 3.22, skewness= $-0.08$, JB= 128.74).

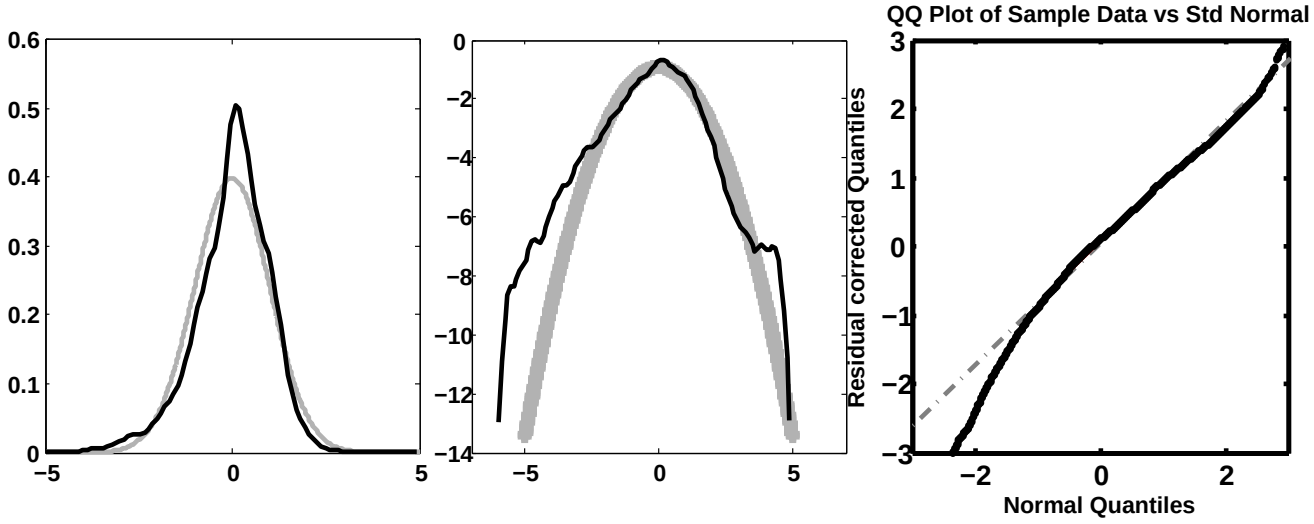


Figure 1: Kernel density estimates (left panel), Log normal densities (middle panel) and QQ-plots (right panel) of normal densities (gray lines) and Kaohsiung standardised residuals (black line)

As in Benth et al. (2007) temperature $T_t$ is decomposed into a seasonality term $\Lambda_t$ and a stochastic part with seasonal volatility $\sigma_t$.

The fitted seasonality trend $\Lambda_t$ and seasonal variance $\sigma_t^2$ are approximated with Fourier series (and an additional GARCH term):

$$\begin{aligned}
\Lambda_t &= a + bt + \sum_{l=1}^{L} c_l \cos\left\{\frac{2\pi(t-d_l)}{l\cdot 365}\right\}, &(1)\\
\sigma^2_{t,FTSG} &= c_{10} + \sum_{l=1}^{L}\left\{c_{2l}\cos\left(\frac{2l\pi t}{365}\right) + c_{2l+1}\sin\left(\frac{2l\pi t}{365}\right)\right\} + \alpha_1(\sigma_{t-1}\eta_{t-1})^2 + \beta_1\sigma^2_{t-1}, &(2)\\
\eta_t &\sim iid(0,1).
\end{aligned}$$

The upper panel of Figure 2 displays the seasonality and deseasonalised residuals over two years in Kaohsiung. The lower panel RHS displays the empirical and seasonal variance function, while the lower panel LHS shows the smoothed seasonal variance function over years. The series expansion (1), (2) failed though in the volatility peak seasons. Even incorporating an asymmetry term for the dip of temperature in winter does not improve the closeness to normality.

One may of course pursue a fine tuning of (1) and (2) with more and more periodic terms but this will increase the number of parameters. We therefore propose a local parametric approach. The seasonality $\Lambda_s$ and $\sigma_s$ are approximated with a Local Linear Regression (LLR) estimator:

$$\arg\min_{e,f} \sum_{t=1}^{365} \left\{\bar{T}_t - e_s - f_s(t-s)\right\}^2 K\Big(\frac{t-s}{h}\Big) \tag{3}$$

$$\arg\min_{g,v} \sum_{t=1}^{365} \left\{\hat{\varepsilon}_t^2 - g_s - v_s(t-s)\right\}^2 K\Big(\frac{t-s}{h}\Big) \tag{4}$$

where $\bar{T}_t$ is the mean (over years) of daily averages temperatures, $\hat{\varepsilon}_t^2$ the squared residual process (after seasonal and intertemporal fitting), $h$ the bandwidth and $K(\cdot)$ is a kernel. Note, that due to the spherical character of the data, the kernel weights in (3), (4) may be calculated from "wrapped around observations" thereby avoiding bias. The estimates $\hat{\Lambda}_s$, $\hat{\sigma}_s^2$ are given by the minimisers $\hat{e}_s$, $\hat{g}_s$ of (3), (4). The upper panel of Figure 2 shows the seasonality in mean and the bottom panel on the RHS the volatility estimated with Fourier series and local linear regression using the quartic kernel. We observe high variance in winter and early summer and low variance in spring and late summer.

The scale correction of the obtained residuals (after seasonal and intertemporal fitting) is apparently not identical over the year. A very structured volatility pattern up to April is followed by a moderately constant period until an increasing peak starting in September. This motivates our research to localise temperature risk. The local smoothness of $\sigma_t^2$ is of course not only a matter of one location (here Kaohsiung) but varies also over the different cities around the world that we are analysing in this study. Our study is local in a double sense: local in time and space. We use adaptive methods to localise the underlying dynamics and with that being able to achieve Gaussian risk factors. This will justify the pricing via standard tools that are based on Gaussian risk drivers. The localisation in time is based on adjusting the smoothing parameter $h$. For a general framework on local parametric approximation we refer to Spokoiny (2009). As a result we obtain better approximations to normality and therefore less biased prices.

This paper is structured as follows. Section 2 describes the localising approach. In section 3, we present the data and conduct the analysis to different cities. Section 4 presents an application

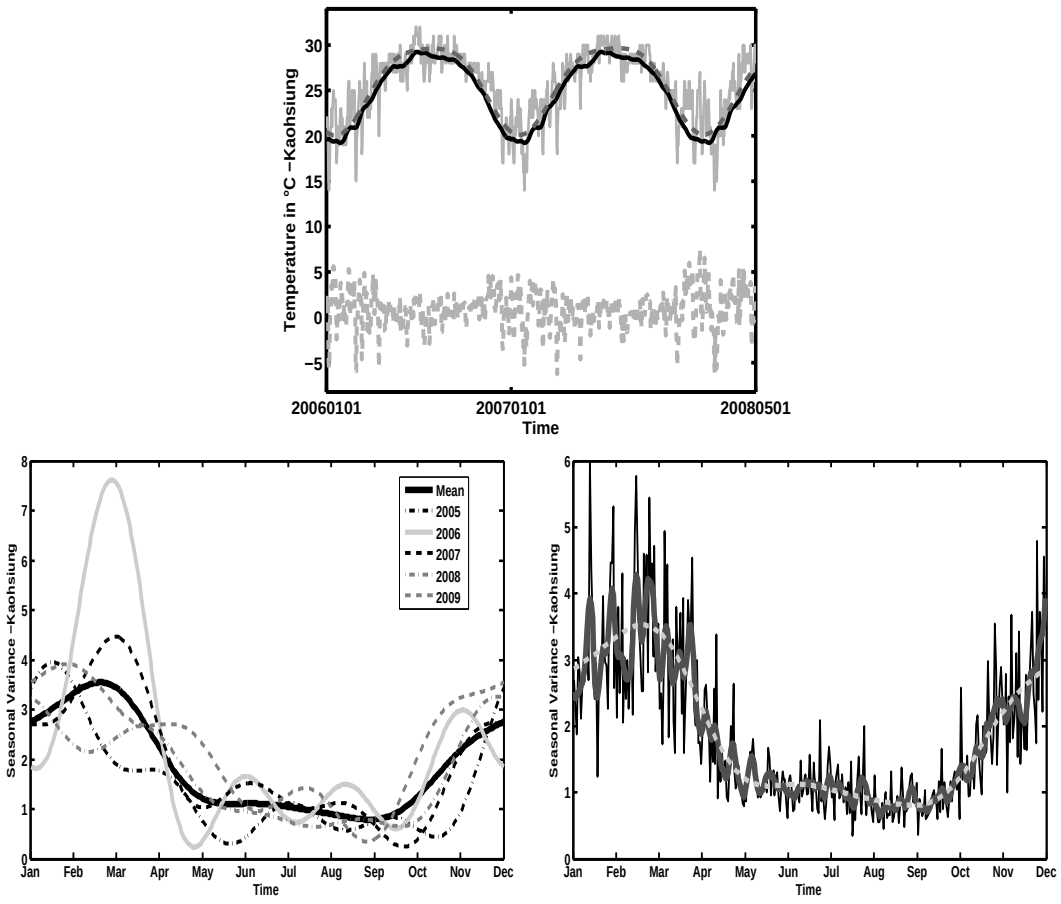


Figure 2: Upper panel: Kaohsiung daily average temperature (black line), Fourier truncated (dotted gray line) and local linear seasonality function (gray line), Residuals in lower part. Lower left panel: Fourier seasonal variation ($\hat{\Lambda}_t$) over time. Lower right panel: Kaohsiung empirical (black line), Fourier (dotted gray line) and local linear (gray line) seasonal variance ($\hat{\varepsilon}_t^2$) function.

where the pricing of weather derivative contract types is presented. Section 5 concludes the paper. All quotations of currency in this paper will be in USD and therefore we will omit the explicit notion of the currency. All the CAT bond computations were carried out in Matlab version 7.6 and R. The temperature data for different cities in US, Europe and Asia were obtained from the National Climatic Data Center (NCDC), the Deutscher Wetterdienst (DWD), Bloomberg Professional Service and the Japanese Meteorological Agency (JMA).

# 2 Model

Let us change our notation from $t \mapsto (t, j)$, with $t = 1, \ldots, \tau = 365$ days, $j = 0, \ldots, J$ years. The time series decomposition we consider is given as:

$$\begin{aligned} X_{365j+t} &= T_{t,j} - \Lambda_t, \\ X_{365j+t} &= \sum_{l=1}^{L} \beta_{lj} X_{365j+t-l} + \varepsilon_{t,j}, \\ \varepsilon_{t,j} &= \sigma_t e_{t,j}, \\ e_{t,j} &\sim \mathsf{N}(0,1), \\ \hat{\varepsilon}_{t,j} &= X_{365j+t} - \sum_{l=1}^{L} \hat{\beta}_{lj} X_{365j+t-l}, \end{aligned} \tag{5}$$

where $T_{t,j}$ is the temperature at day $t$ in year $j$, $\Lambda_t$ denotes the seasonality effect and $\sigma_t$ the seasonal volatility. Motivation of this modeling approach can be found in Diebold and Inoue (2001). Later studies like e.g. Campbell and Diebold (2005) and Benth et al. (2007) have provided evidence that the parameters $\beta_{lj}$ are likely to be $j$ independent and hence estimated consistently from a global autoregressive process model $AR(L_j)$ with $L_j = L$. Since the stylised facts of temperature are re-occurring every year, our focus is on flexible estimation of $\Lambda_t$ and $\sigma_t^2$, see Figure 2.

The seasonal trend function $\Lambda_t$ and the seasonal variance function $\sigma_t^2$ affect the Gaussianity of the resulting normalised residuals. The commonly used approaches 1. truncated Fourier series, 2. local polynomial regression are both too restrictive and do not fit the data well since they are not yielding normal risk factors. These observations motivate us to consider a more flexible approach. The main idea is to fit a simple parametric model locally for the trend and variance with adaptively chosen window sizes. Specifically, we use kernel smoothing and adopt an adaptive technique to choose the bandwidth over days. Other examples of this technique can be found in Cízek, Härdle and Spokoiny (2009) and Chen, Härdle and Pigorsch (2010).

## 2.1 How does the adaptation work?

The time series $T_{t,j}$ are approximated at a fixed time point $s \in [1, 365]$. Our goal is to find a local window that follows certain optimality properties to be defined below. Specifically, for a specified weight sequence, we conduct a sequential LRT to choose an appropriate bandwidth. Different procedures of estimating seasonality and volatility are studied. Suppose that the object to be approximated is the seasonal variance $\theta(t) = \{\sigma_t^2\}$. A weighted maximum likelihood approach is

given by:

$$\begin{aligned}\tilde{\theta}_k(s) &\stackrel{\text{def}}{=} \arg\max_{\theta\in\Theta} L\{W^k(s),\theta\} \\ &= \arg\min_{\theta\in\Theta} \sum_{t=1}^{365}\sum_{j=0}^{J}\{\log(2\pi\theta)/2 + \hat{\varepsilon}_{t,j}^2/2\theta\}w(s,t,h_k), \end{aligned} \tag{6}$$

with the "localising scheme" $W^k(s) = \{w(s,1,h_k), w(s,2,h_k), \ldots, w(s,365,h_k)\}^\top$, where $w(s,t,h_k) = h_k^{-1}K\{(s-t)/h_k\}$, $k = 1,\ldots,K$, $h_1 < h_2 < h_3 < \ldots < h_K$ the prescribed sequence of bandwidths, and $K(u) = 15/16(1-u^2)^2\mathbf{I}(|u| \le 1)$ (quartic kernel).

The explicit solution of (6) is given by:

$$\begin{aligned}\tilde{\theta}_k(s) &= \sum_{t,j}\hat{\varepsilon}_{t,j}^2 w(s,t,h_k)/\sum_{t,j} w(s,t,h_k) \\ &= \sum_{t}\hat{\varepsilon}_{t}^2 w(s,t,h_k)/\sum_{t} w(s,t,h_k),\end{aligned}$$

with

$$\hat{\varepsilon}_t^2 \stackrel{\text{def}}{=} (J+1)^{-1}\sum_{j=0}^{J}\hat{\varepsilon}_{t,j}^2.$$

>From a smoothing perspective we are in a comfortable situation here since the boundary bias is not an issue, as we are dealing with a periodic function $\theta(t) = \theta(t+365)$. We use mirrored observations: assume $h_K < 365/2$, then the observation set, for example for the seasonal volatility, is extended to $\hat{\varepsilon}_{-364}^2, \hat{\varepsilon}_{-363}^2, \ldots, \hat{\varepsilon}_0^2, \hat{\varepsilon}_1^2, \ldots, \hat{\varepsilon}_{730}^2$, where

$$\begin{aligned}\hat{\varepsilon}_t^2 &\stackrel{\text{def}}{=} \hat{\varepsilon}_{365+t}^2, -364 \le t \le 0, \\ \hat{\varepsilon}_t^2 &\stackrel{\text{def}}{=} \hat{\varepsilon}_{t-365}^2, 366 \le t \le 730.\end{aligned}$$

Since the location $s$ is fixed, we drop $s$ for the simplicity of notation.

For $\ell < k$, the accuracy of the estimation is measured by the fitted likelihood ratio (LR):

$$L(W^\ell, \tilde{\theta}_\ell, \tilde{\theta}_k) \stackrel{\text{def}}{=} L(W^\ell, \tilde{\theta}_\ell) - L(W^\ell, \tilde{\theta}_k).$$

The volatility $\sigma_t$ or trend $\Lambda_t$ estimation happens within an exponential family, so LR can be written in closed form, Polzehl and Spokoiny (2006):

$$\begin{aligned}L(W^k, \tilde{\theta}_k, \theta^*) &\stackrel{\text{def}}{=} N_k\mathcal{K}(\tilde{\theta}_k, \theta^*) \\ &= -\{\log(\tilde{\theta}_k/\theta^*) + 1 - \theta^*/\tilde{\theta}_k\}/2,\end{aligned} \tag{7}$$

where $N_k = J\sum_{t=1}^{365} w(s,t,h_k)$ and $\mathcal{K}(\tilde{\theta}_k, \theta^*)$ is the Kullback-Leibler divergence between two normal distributions with variances $\tilde{\theta}_k$ and $\theta^*$. Note that (7) is the divergence in the volatility case. For trend estimation, it has to be replaced by $(\tilde{\theta}_k - \theta^*)/(2\sigma^2)$.

The Kullback-Leibler divergence of two distributions with densities $p(x)$ and $q(x)$ is defined as:

$$\mathcal{K}\left\{p(x), q(x)\right\} \stackrel{\text{def}}{=} \mathsf{E}_{p(.)} \log \frac{p(x)}{q(x)}.$$

To guarantee the feasibility of the tests, we need moment bounds and confidence sets for LR, which guarantee that the MLE is concentrated in the level set of the likelihood ratio process around the true parameter. For the volatility case, see Polzehl and Spokoiny (2006); for the trend case, see Mercurio and Spokoiny (2004).

**Theorem 2.1** *[Spokoiny (2009)] Assuming that $\theta(t) = \theta^*$ for any $t \in [1, 365]$, then for $\mathfrak{z} > 0$ and $k \in 1, \ldots, K, r > 0$, denote $\mathrm{P}_{\theta^*}(.)$ as the measure corresponding to (6). We obtain:*

$$\mathrm{P}_{\theta^*}\left\{L(W^k, \tilde{\theta}_k, \theta^*) > \mathfrak{z}\right\} \leq 2\exp\left(-\mathfrak{z}\right) \tag{8}$$

*and a risk bound for a power loss function:*

$$\mathsf{E}_{\theta^*}|L(W^k, \tilde{\theta}_k, \theta^*)|^r \leq \mathfrak{r}_r, \tag{9}$$

*where $\mathfrak{r}_r = 2r\int_{\mathfrak{z}\geq 0} \mathfrak{z}^{r-1}\exp(-\mathfrak{z})d\mathfrak{z}$. This polynomial bound applies to all localising schemes $W^k$ simultaneously.*

The risk bound (9) allows us to define likelihood based confidence sets since together with (8) it tells us that the likelihood process is stochastically bounded. Define therefore confidence sets with critical values $\mathfrak{z}_k$ to level $\alpha$:

$$\mathfrak{E}_{\alpha,k} = \{\theta : L(W^k, \tilde{\theta}_k, \theta) \leq \mathfrak{z}_k\}. \tag{10}$$

Equipped with confidence sets (10), we launch the Local Model Selection (LMS) algorithm:

- Fix a point $s \in \{1, 2, \ldots, 365\}$.
- Start with the smallest interval $h_1$: $\hat{\theta}_1 = \tilde{\theta}_1$
- For $k \geq 2$, $\tilde{\theta}_k$ is accepted and $\hat{\theta}_k = \tilde{\theta}_k$ if $\tilde{\theta}_{k-1}$ was accepted and $\tilde{\theta}_\ell \in \mathfrak{E}_{\alpha,k}, \forall \ell = 1, \ldots, k-1$, i.e.

  $$L(W^k, \tilde{\theta}_\ell, \tilde{\theta}_k) \leq \mathfrak{z}_\ell, \forall \ell = 1, \ldots, k-1.$$

  Otherwise, set $\hat{\theta}_k = \hat{\theta}_{k-1}$, where $\hat{\theta}_k$ is the latest accepted after first $k$ steps.
- Define $\hat{k}$ as the $k$th step we stopped, and $\hat{\theta}_\ell = \tilde{\theta}_{\hat{k}}, \ell \geq k$.

The LMS algorithm is illustrated in Figure 3. For every estimate $\tilde{\theta}_k$ the corresponding confidence set is shown. If the horizontal line originating $\tilde{\theta}_k$ does not cross all the preceding intervals then the selection algorithm terminates.

A further integrated approach is to consider an iterative algorithm to cope with heteroscedasticity in the corrected residuals after seasonality in mean and variance component varies between estimating the seasonal component and the variance $\theta(t) = \{\Lambda_t, \sigma_t^2\}$. The procedure is:

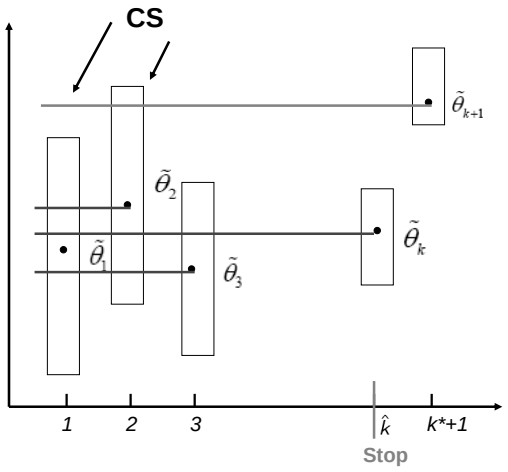


Figure 3: Localised model selection (LMS)

Step 1. Estimate $\hat{\beta}$ in an initial $\Lambda_t^0$ using a truncated Fourier series or any other deterministic function;

Step 2. For fixed $\hat{\Lambda}_{s,\nu} = \{\hat{\Lambda}'_{s,\nu}, \hat{\Lambda}''_{s,\nu}\}^\top, s = \{1, \ldots, 365\}$ from last step $\nu$, and fixed $\hat{\beta}$, get $\hat{\sigma}^2_{s,\nu+1}$ by

$$\begin{aligned}\hat{\sigma}^2_{s,\nu+1} &= \arg\min_{\sigma^2} \sum_{t=1}^{365}\sum_{j=0}^{J}[\{T_{365j+t} - \hat{\Lambda}'_{s,\nu} - \hat{\Lambda}''_{s,\nu}(t-s) \\ &- \sum_{l=1}^{L}\hat{\beta}_l X_{365j+t-l}\}^2/2\sigma^2 + \log(2\pi\sigma^2)/2]w(s,t,h'_k);\end{aligned}$$

Step 3. For fixed $\hat{\sigma}^2_{s,\nu+1}$ and $\hat{\beta}$, we estimate $\hat{\Lambda}_{s,\nu+1}, s = \{1, \ldots, 365\}$ via another local adaptive procedure:

$$\hat{\Lambda}_{s,\nu+1} = \arg\min_{\{\Lambda',\Lambda''\}^\top} \sum_{t=1}^{365}\sum_{j=0}^{J}\left\{T_{365j+t} - \Lambda' - \Lambda''(t-s) - \sum_{l=1}^{L}\hat{\beta}_l X_{365j+t-l}\right\}^2 w(s,t,h'_k)/2\hat{\sigma}^2_{s,\nu+1},$$

where $\{h'_1, h'_2, h'_3, \ldots, h'_{K'}\}$ is a sequence of bandwidths;

Step 4. Repeat steps 2 and 3 till both $|\hat{\Lambda}_{t,\nu+1} - \hat{\Lambda}_{t,\nu}| < \pi_1$ and $|\hat{\sigma}^2_{t,\nu+1} - \hat{\sigma}^2_{t,\nu}| < \pi_2$ for some constants $\pi_1$ and $\pi_2$.

Our empirical implementation suggests that one iteration is enough.

The LMS methods requires critical values $\mathfrak{z}_k$, which define the significance for the LRT statistics $L(W^\ell, \tilde{\theta}_\ell, \tilde{\theta}_k)$ or alternatively speaking the length of the confidence interval (see (8)) at each step. The critical values are calibrated from the "propagation condition" below which ensures a desired level of type one error. To be more specific, for every step $k$, define $\hat{\theta}_k$ as the "survived estimator" after the $k$th step (if the estimator is not rejected up to step $k$, then $\hat{\theta}_k = \tilde{\theta}_k$, else if the estimator has been rejected at step $l < k$, then $\hat{\theta}_k = \tilde{\theta}_l$). Measure the closeness of $\tilde{\theta}_k$ and $\hat{\theta}_k$ by:

$$\mathsf{E}_{\theta^*}|L(W^k, \tilde{\theta}_k, \hat{\theta}_k)|^r \leq \alpha\mathfrak{r}_r \tag{11}$$

for $k = 1, \ldots, K$ with $\mathfrak{r}_r$ the parametric risk bound in (9) and $\alpha$ a control parameter corresponding to the type one error. In fact

$$\mathsf{E}_{\theta^*}|L(W^k, \tilde{\theta}_k, \hat{\theta}_k)|^r \to \mathrm{P}_{\theta^*}(\tilde{\theta}_k \neq \hat{\theta}_k)$$

for $r \to 0$, therefore $\alpha$ can be interpreted as a false alarm probability.

More precisely if step $k$ is accepted as described in Figure 3 then $\tilde{\theta}_k = \hat{\theta}_k$ and the nonzero loss $\mathsf{E}_{\theta^*} L(W^k, \tilde{\theta}_k, \hat{\theta}_k)$ can only occur if the estimator has been rejected before or at step $k$, which under the homogeneous parametric model case, is denoted as "false alarm".

With the "propagation condition" (13) below, critical values are constructed.

- Consider first $\mathfrak{z}_1$ and let $\mathfrak{z}_2 = \mathfrak{z}_3 = \ldots = \mathfrak{z}_{K-1} = \infty$. This leads to the estimates $\hat{\theta}_k(\mathfrak{z}_1)$ and the value $\mathfrak{z}_1$ is selected as the minimal one for which

$$\sup_{\theta^*} \mathsf{E}_{\theta^*}|L\{W^k, \tilde{\theta}_k, \hat{\theta}_k(\mathfrak{z}_1)\}| \leq \frac{\alpha \mathfrak{r}_r}{K-1}, k = 2, \ldots, K. \tag{12}$$

- Suppose $\mathfrak{z}_1, \ldots, \mathfrak{z}_{k-1}$ have been fixed, and set $\mathfrak{z}_k = \ldots = \mathfrak{z}_{K-1} = \infty$. With estimate $\hat{\theta}_m(\mathfrak{z}_1, \ldots, \mathfrak{z}_k)$ for $m = k+1, \ldots, K$. select $\mathfrak{z}_k$ as the minimal value which fulfills

$$\sup_{\theta^*} \mathsf{E}_{\theta^*}|L\{W^m, \tilde{\theta}_m, \hat{\theta}_m(\mathfrak{z}_1, \ldots, \mathfrak{z}_k)\}|^r \leq \frac{k\alpha \mathfrak{r}_r}{K-1} \tag{13}$$

  for $m = k+1, \ldots, K$.

Inequality (12) describes the impact of the $k$ critical values to the risk, while the factor $\frac{k\alpha}{K-1}$ in (13) ensures that every $\mathfrak{z}_k$ has the same impact. The values of $(\alpha, r, h_1, \ldots, h_K)$ are prespecified hyper-parameters of which robustness and sensitivity issues will be discussed in Section 3. The following theorem provides insight into the form of $\mathfrak{z}_k$.

**Theorem 2.2** *[Spokoiny (2009)] Suppose that* $0 < h_{k-1}/h_k < 1$ *and* $\theta(t) = \theta^*$ *for all* $t \in [0, 365]$. *An upper bound for the critical values* $\mathfrak{z}_k$ *is given by:*

$$\mathfrak{z}_k = a_0 \log K + 2\log(nh_k/\alpha) + 2r\log(h_K/h_k)$$

*where* $a_0 > 0$ *is a constant.*

A risk bound for a global model ($\theta(t) = \theta^*$) has been given in (11). This may now be extended to the nonparametric setting via the "Small Modeling Bias (SMB)" condition:

$$\Delta(\theta) \stackrel{\text{def}}{=} \sum_{t=1}^{365} \mathcal{K}(\theta_t, \theta)\, \mathbf{I}\{w(s, t, h_k) > 0\} \leq \Delta, \forall k < k^*, \tag{14}$$

where $k^*$ is the maximum $k$ satisfying (14), also called "oracle".

The estimation risk for the function $\theta(t)$ is described for $k \leq k^*$ by the "propagation" property:

$$\mathsf{E}_{\theta(\cdot)} \log\{1 + |L(W^k, \tilde{\theta}_k, \hat{\theta}_k)|^r / \mathfrak{r}_r\} \leq \Delta + \alpha.$$

An estimate for $k^*$ is desired. The adaptive estimate $\hat{\theta}_{\hat{k}}$ will in fact enjoy this property as we show below. The estimate $\hat{\theta}_{\hat{k}}$ behaves similarly to the oracle estimate $\tilde{\theta}_{k^*}$ since it is "stable" in the sense that even if the described selection scheme overshoots $k^*$, the resulting estimate $\hat{\theta}_{\hat{k}}$ is still close to the oracle $\tilde{\theta}_{k^*}$. This may be expressed as that the attained quality of estimation during "propagation" is not lost at further steps:

$$L(W^{k^*}, \tilde{\theta}_{k^*}, \hat{\theta}_{\hat{k}})\, \mathbf{I}\{\hat{k} > k^*\} \leq \mathfrak{z}_{k^*}.$$

A combination of the propagation and stability property then leads to the "oracle" property:

$$\begin{aligned}
\mathsf{E}_{\theta(\cdot)} \log\left\{1 + \frac{|L(W^{k^*}, \tilde{\theta}_{k^*}, \theta)|^r}{\mathfrak{r}_r}\right\} &\leq \Delta + 1, \\
\mathsf{E}_{\theta(\cdot)} \log\left\{1 + \frac{|L(W^{k^*}, \tilde{\theta}_{k^*}, \hat{\theta}_{\hat{k}})|^r}{\mathfrak{r}_r}\right\} &\leq \Delta + \alpha + \log\left\{1 + \frac{\mathfrak{z}_{k^*}}{\mathfrak{r}_r}\right\},
\end{aligned}$$

for $\theta \in \Theta$ with $\Delta(W^k, \theta) \leq \Delta$ and $k \leq k^*$. This means that the risk of estimating adaptively is composed into three parts: the SMB, the false alarm rate and a small term corresponding to the overshooting risk.

# 3 Empirical analysis

We conduct an empirical analysis of temperature patterns over different cities (Figure 4). The data set contains daily average temperatures for different cities in Europe, Asia and US: Atlanta, Beijing, Berlin, Essen, Houston, Kaoshiung, New York, Osaka, Portland, Taipei, Tokyo. The summary of the data and characteristics can be seen in Table 1.


Figure 4: Map of locations where temperature are collected

We first check seasonality, intertemporal correlation and seasonal variation. Table 2 provides the coefficients of the Fourier truncated seasonal function (1) for some cities for different time periods. The coefficient $a$ can be seen as the average temperature, the coefficient $b$ as an indicator for global warming. The latter coefficients are stable even when the estimation is done in a window length of 10 years. In the sense of capturing volatility peak seasons, the left panel of Figure 5 visualises the power of capturing volatility peak seasons by the seasonal local smoother (3) using the quartic kernel over the estimates modeled under Fourier truncated series (1).

| City | Period | ADF | KPSS | $AR(3)$ | | | $CAR(3)$ | | |
|---|---|---|---|---|---|---|---|---|---|
| | | $\hat{\tau}$ | $\hat{k}$ | $\beta_1$ | $\beta_2$ | $\beta_3$ | $\alpha_1$ | $\alpha_2$ | $\alpha_3$ |
| Atlanta | 19480101-20081204 | -55.55+ | 0.21*** | 0.96 | -0.38 | 0.13 | 2.03 | 1.46 | 0.28 |
| Beijing | 19730101-20090831 | -30.75+ | 0.16*** | 0.72 | -0.07 | 0.05 | 2.27 | 1.63 | 0.29 |
| Berlin | 19480101-20080527 | -40.94+ | 0.13** | 0.91 | -0.20 | 0.07 | 2.08 | 1.37 | 0.20 |
| Essen | 19700101-20090731 | -23.87+ | 0.11* | 0.93 | -0.21 | 0.11 | 2.06 | 1.34 | 0.16 |
| Houston | 19700101-20081204 | -38.17+ | 0.05* | 0.90 | -0.39 | 0.15 | 2.09 | 1.57 | 0.33 |
| Kaohsiung | 19730101-20091210 | -37.96+ | 0.05* | 0.73 | -0.08 | 0.04 | 2.26 | 1.60 | 0.29 |
| New York | 19490101-20081204 | -56.88+ | 0.08* | 0.76 | -0.23 | 0.11 | 2.23 | 1.69 | 0.34 |
| Osaka | 19730101-20090604 | -18.65+ | 0.09* | 0.73 | -0.14 | 0.06 | 2.26 | 1.68 | 0.34 |
| Portland | 19480101-20081204 | -45.13+ | 0.05* | 0.86 | -0.22 | 0.08 | 2.13 | 1.48 | 0.26 |
| Taipei | 19920101-20090806 | -32.82+ | 0.09* | 0.79 | -0.22 | 0.06 | 2.20 | 1.63 | 0.36 |
| Tokyo | 19730101-20090831 | -25.93+ | 0.06* | 0.64 | -0.07 | 0.06 | 2.35 | 1.79 | 0.37 |

Table 1: ADF and KPSS-Statistics, coefficients of the autoregressive process $AR(3)$ and continuous autoregressive model $CAR(3)$ model for the detrended daily average temperatures time series for different cities. +0.01 critical values, * 0.1 critical value, **0.05 critical value, ***0.01 critical value.

| City | Period | $\hat{a}$ | $\hat{b}$ | $\hat{c}_1$ | $\hat{d}_1$ | $\hat{c}_2$ | $\hat{d}_2$ | $\hat{c}_3$ | $\hat{d}_3$ |
|---|---|---|---|---|---|---|---|---|---|
| Berlin | (19480101-20080527) | 9.2173 | 0.0000 | 9.8932 | -157.9123 | 0.2247 | 261.2850 | 0.1591 | -127.7303 |
| | (19730101-20080527) | 9.3050 | 0.0001 | 10.0070 | -161.2493 | 0.4601 | -66.0530 | -0.3723 | -416.4776 |
| | (19730101-20080527) | 9.3050 | 0.0001 | 10.0070 | -161.2493 | 0.4601 | -66.0530 | -0.3723 | -416.4776 |
| | (19830101-20080527) | 9.4581 | 0.0001 | 10.0969 | -161.7129 | 0.5205 | -51.9929 | 0.3734 | 42.0874 |
| | (19930101-20080527) | 9.5923 | 0.0002 | 10.1995 | -162.9774 | 0.6564 | -37.1548 | 0.4241 | 41.9970 |
| | (20030101-20080527) | 9.6948 | 0.0007 | 10.1954 | -162.3343 | 0.5554 | -43.2293 | 0.3269 | 1.5998 |
| Kaohsiung | (19730101-20081231) | 24.2289 | 0.0001 | 0.9157 | -145.6337 | -4.0603 | -78.1426 | -1.0505 | 10.6041 |
| | (19730101-19821231) | 24.4413 | 0.0001 | 2.1112 | -129.1218 | -3.3887 | -91.1782 | -0.8733 | 20.0342 |
| | (19830101-19921231) | 25.0616 | 0.0003 | 2.0181 | -135.0527 | -2.8400 | -89.3952 | -1.0128 | 20.4010 |
| | (19930101-20021231) | 25.3227 | 0.0003 | 3.9154 | -165.7407 | -0.7405 | -51.4230 | -1.1056 | 19.7340 |
| New-York | (19490101-20081204) | 53.1473 | 0.0001 | 18.6810 | -143.4051 | -3.3872 | 271.5072 | -0.4203 | -16.3125 |
| | (19730101-20081204) | 53.6992 | 0.0001 | 18.0092 | -148.4124 | -3.5236 | 279.6876 | -0.4756 | -21.8090 |
| | (19730101-19821204) | 53.6037 | -0.0000 | 17.7446 | -155.2453 | -3.7769 | 289.7932 | -0.8326 | -4.2257 |
| | (19830101-19921204) | 54.8740 | -0.0003 | 17.6924 | -152.7461 | -3.4245 | 284.6412 | -0.4933 | -218.9204 |
| | (19930101-20021204) | 53.8050 | 0.0003 | 17.6942 | -153.3997 | -3.4246 | 285.7958 | 0.5753 | -315.2792 |
| | (20030101-20081204) | 52.9177 | 0.0012 | 17.8425 | -151.2977 | -3.8837 | 287.2022 | -0.1290 | -216.7298 |
| Tokyo | (19730101-20081231) | 15.7415 | 0.0001 | 8.9171 | -162.3055 | -2.5521 | -7.8982 | -0.7155 | -15.0956 |
| | (19730101-19821231) | 15.8109 | 0.0001 | 9.2855 | -162.6268 | -1.9157 | -16.4305 | -0.5907 | -13.4789 |
| | (19830101-19921231) | 15.4391 | 0.0004 | 9.4022 | -162.5191 | -2.0254 | -4.8526 | -0.8139 | -19.4540 |
| | (19930101-20021231) | 16.4284 | 0.0001 | 8.8176 | -162.2136 | -2.1893 | -17.7745 | -0.7846 | -22.2583 |
| | (20030101-20081231) | 16.4567 | 0.0001 | 8.5504 | -162.0298 | -2.3157 | -18.3324 | -0.6843 | -16.5381 |

Table 2: Seasonality estimates $\hat{\Lambda}_t$ of daily average temperatures in Asia. All coefficients are nonzero at 1% significance level. Data source: Bloomberg.

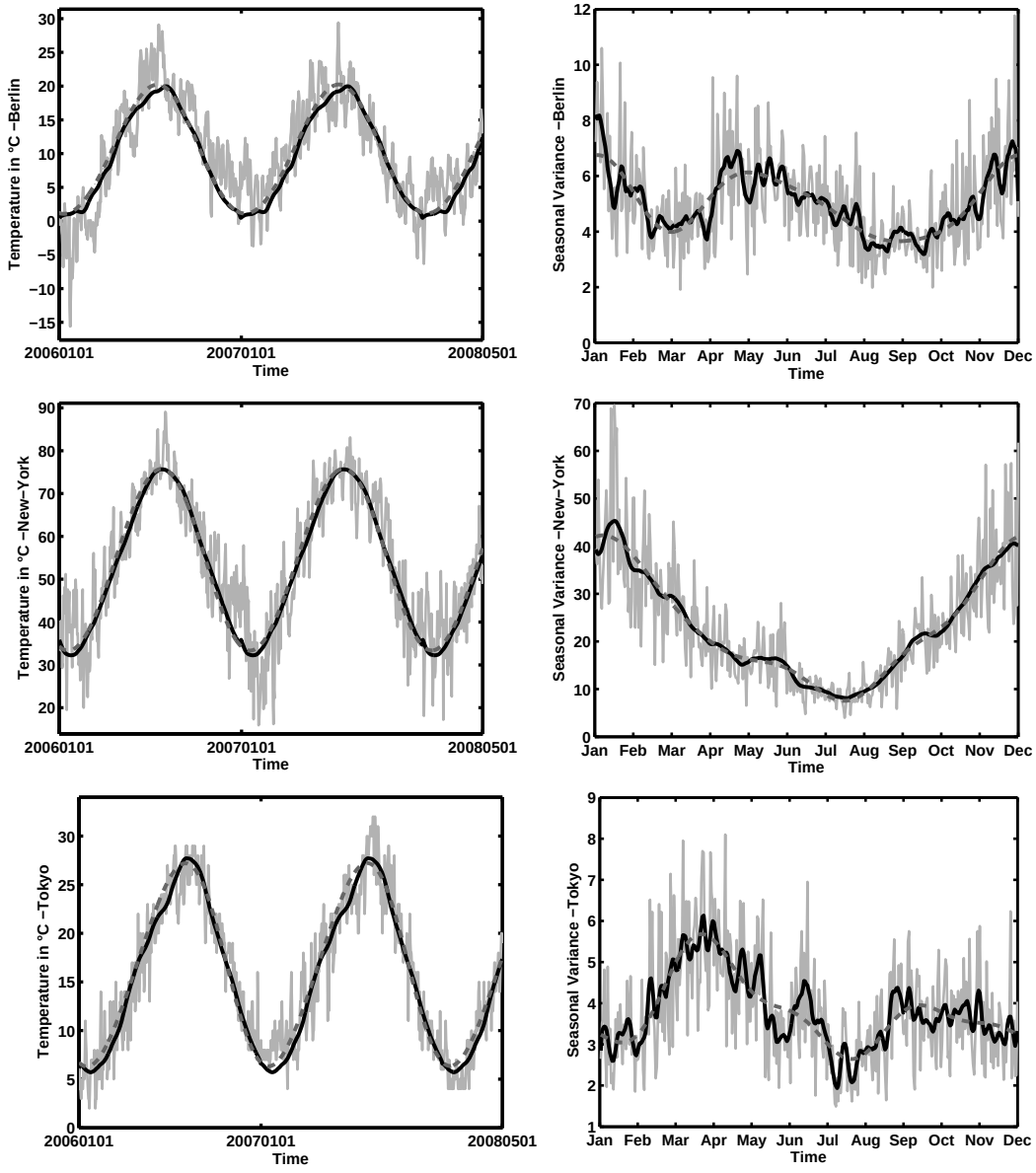


Figure 5: The empirical (black line), the Fourier truncated (dotted gray line) and the the local linear (gray line) seasonal mean (left panel) and variance component (right panel) using Quartic kernel and bandwidth $h = 4.49$.

| City | Corrected residuals with Fourier $\frac{\hat{\varepsilon}_t}{\hat{\sigma}_{t,FTSG}}$ | | | | | Corrected residuas with Local smoother $\frac{\hat{\varepsilon}_t}{\hat{\sigma}_{t,LLR}}$ | | | | |
|---|---|---|---|---|---|---|---|---|---|---|
| | JB | Kurtosis | Skewness | KS | AD | JB | Kurtosis | Skewness | KS | AD |
| Berlin | 304.77 | 3.54 | -0.08 | 0.01 | 7.65 | 279.06 | 3.52 | -0.08 | 0.01 | 7.29 |
| New-York | 403.39 | 3.47 | -0.23 | 0.02 | 23.22 | 375.50 | 3.45 | -0.228 | 0.02 | 21.74 |
| Kaohsiung | 2753.00 | 4.68 | -0.71 | 0.06 | 79.93 | 2252.50 | 4.52 | -0.64 | 0.06 | 79.18 |
| Tokyo | 133.26 | 3.44 | -0.10 | 0.02 | 8.06 | 148.08 | 3.44 | -0.13 | 0.02 | 10.31 |

Table 3: Skewness, kurtosis, Jarque Bera (JB), Kolmogorov Smirnov (KS) and Anderson Darling (AD) test statistics (365 days) of corrected residuals.

After removing the local linear seasonal mean (3) from the daily average temperatures ($X_t = T_t - \Lambda_{t,LNN}$), we check that $X_t$ is a stationary process with the Augmented Dickey-Fuller (ADF) and the KPSS tests. The analysis of the partial autocorrelations and Akaike's Information criterion (AIC) suggest that a simple $AR(3)$ model fits the temperature evolution well. Table 1 presents the results of the stationarity tests as well as the coefficients of the fitted $AR(3)$. The empirical seasonal variation (square residuals after seasonal and intertemporal fitting), the seasonal variation curves (2) and (4) are displayed on the right panel in Figure 5, while the descriptive statistics for the residuals after correcting by seasonality are given in Table 3. Both seasonal volatility estimators lead to heavy tail distributions of corrected residuals and negative skewness.

The adjustment in the smoothing parameter $h$ will provide the localisation in time. The bandwidth sequences are selected from four candidates: $(3, 5, 7, 9, 11, 13, 15)$, $(3, 5, 8, 12, 17, 23, 30)$, $(5, 7, 10, 14, 19, 25, 32)$, $(7, 9, 11, 14, 17, 10, 24)$. The candidates are chosen according to the lowest Anderson Darling statistic. The best candidate for bandwidth sequence is that one that yields a residual distribution close to normality. Smoothing the bandwidths selected at discrete points, gives yet another adaptive estimator.

The critical values (CV) as calibrated from (12) and (13) are given in Figure 6. The left side provides CVs simulated from a sample of $10^3$ observations for a quartic kernel for both mean and volatility with $\theta^* = 1$, $r = 0.5$ and different values of significance level $\alpha$. The CVs for different bandwidth sequences are displayed in the right side of Figure 6. The CVs, as one observes, are insensitive to the choice of $r$ and $\alpha$.

A one year short period is considered in the first place for demonstration purpose, while later we show how the results change with different time length periods. Figures 7, 8, 9 and 10 present general results for different cities under different adaptive localising schemes for seasonal mean (Me) and seasonal volatility (Vo): with fixed bandwidth curve (fi), adaptive bandwidth curve (ad) and adaptive smoothed bandwidth (ads) for different time intervals. The seasonal mean is estimated jointly over the years, using $\alpha = 0.3$ and power level $r = 0.5$. The upper panel of each volatility plot on Figures 7-10 shows the sequence of bandwidths and the smoothed bandwidth; the bottom panel displays the variance estimation with fixed bandwidth (dashed line), smoothed adaptive bandwidth (dotted line) and adaptive bandwidth (dot-dashed line). In all countries, one observes significant differences between the estimates. When smoothing the discrete bandwidths over time, the estimated variance curves are smoother. In particular, in cities like Kaohsiung and New York, one observes more variation of the seasonal variance curves during peak seasons (winter and summer times). The triangles and circles in the bottom panel of each volatility plot helps us to trace the source of non-normality over time, since they corresponds to 10 dots of the upper and lower tails of the QQ-plots of square residuals respectively (see Figure 11 for Berlin results).

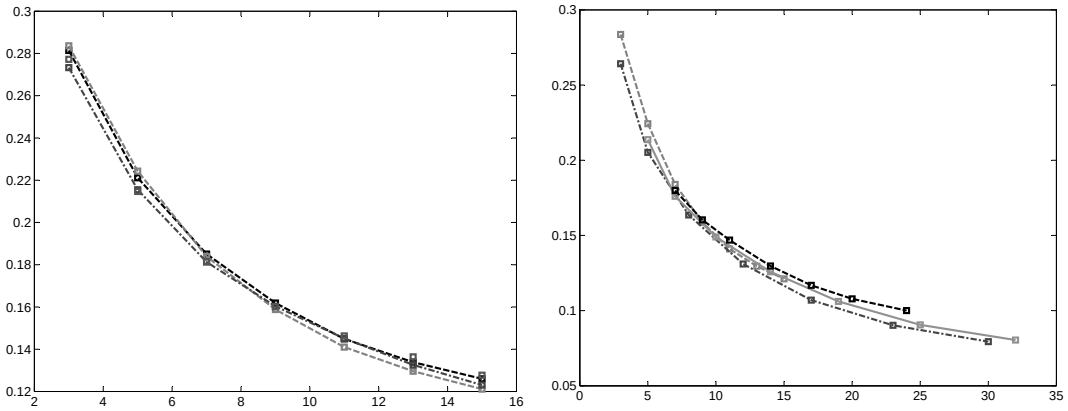


Figure 6: Simulated CV for likelihood of seasonal volatility (6) with $\theta^* = 1$, $r = 0.5$, $MC = 5000$ with $\alpha = 0.3$ (gray dotted line), 0.5 (black dotted line), 0.8 (dark gray dotted line) (left), with different bandwidth sequences (right).

Left top plots of Figures 7- 10 show the mean case. Different from the seasonal variance function, we do not observe a big variation of smoothness in the mean function. One can see that in all cities, the bandwidths are varying over the yearly cycle with a slight degree of non homogeneity for Kaoshiung.

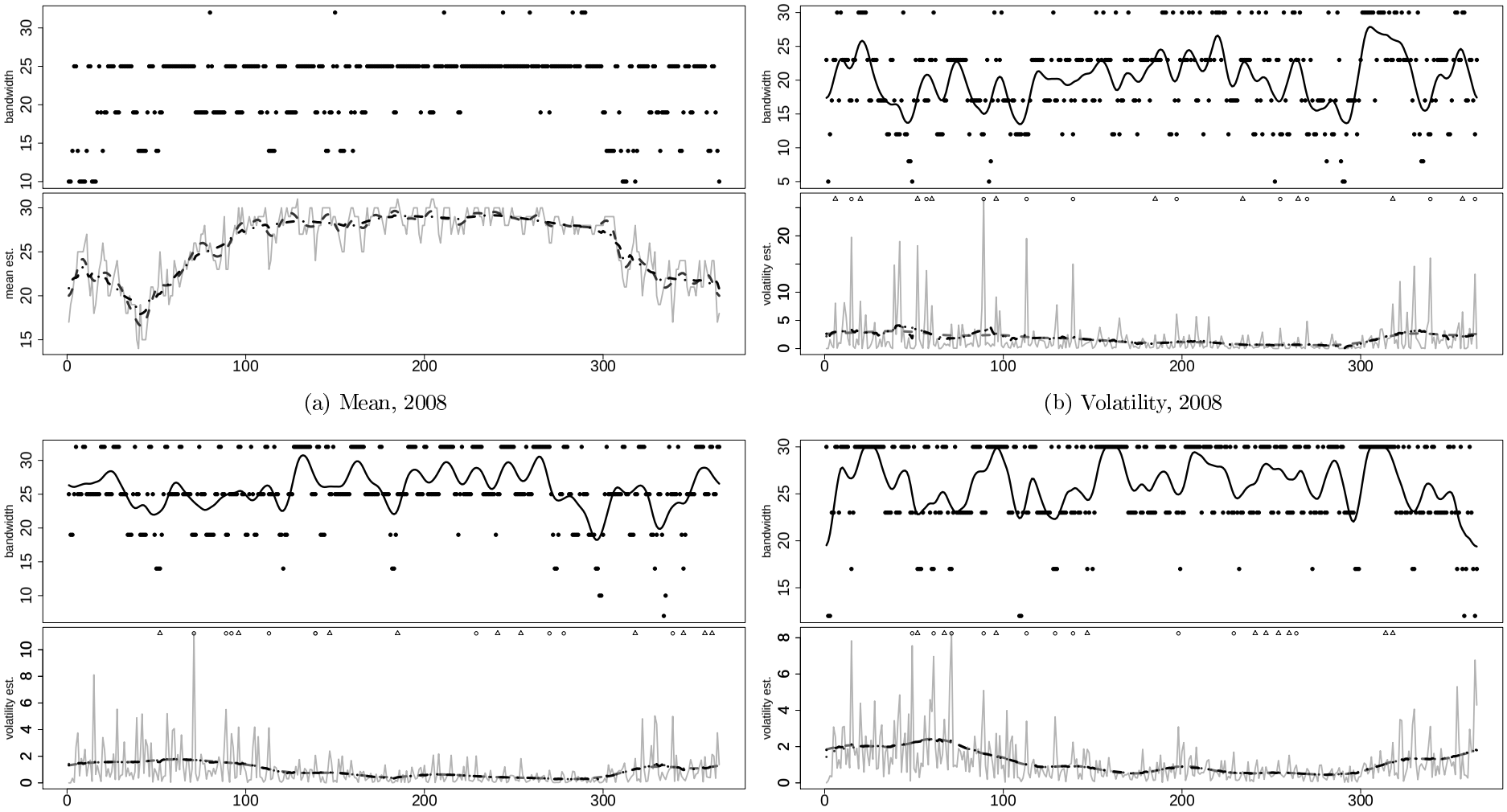


(a) Mean, 2008

(b) Volatility, 2008

(c) Volatility, 2006-2008

(d) Volatility, 2004-2008

Figure 7: Estimation of mean and variance for Kaohsiung. In each figure sequence (also smoothed for volatility) of bandwidths (upper panel), nonparametric function estimation (solid grey line), with fixed bandwidth (dashed line), adaptive bandwidth (dot-dashed line) and smoothed adaptive bandwidth (dotted line) (bottom panel of each figure).

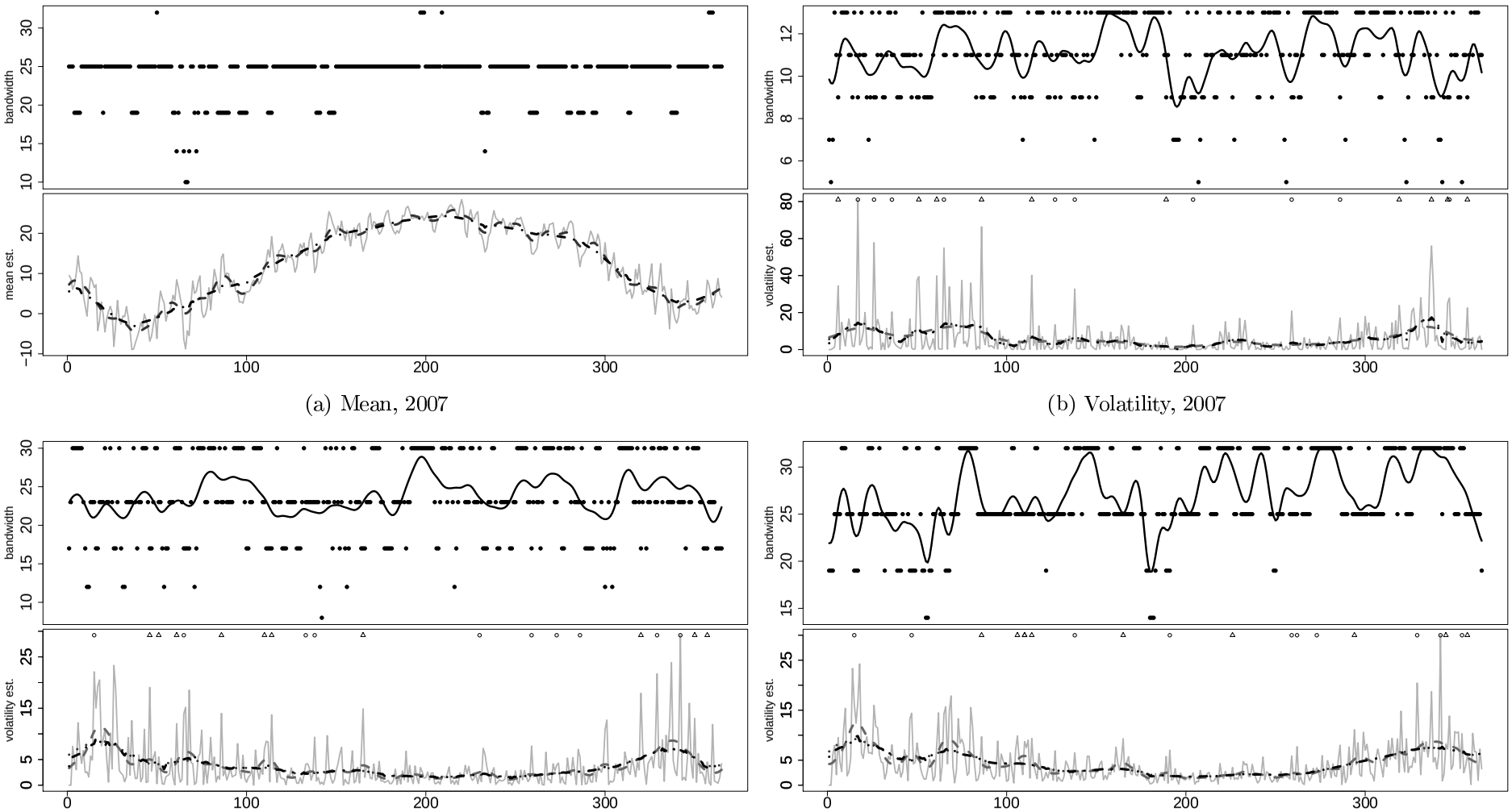


(a) Mean, 2007

(b) Volatility, 2007

(c) Volatility, 2005-2007

(d) Volatility, 2003-2007

Figure 8: Estimation of mean and variance for New-York. In each figure sequence (also smoothed for volatility) of bandwidths (upper panel), nonparametric function estimation (solid grey line), with fixed bandwidth (dashed line), adaptive bandwidth (dot-dashed line) and smoothed adaptive bandwidth (dotted line) (bottom panel of each figure).

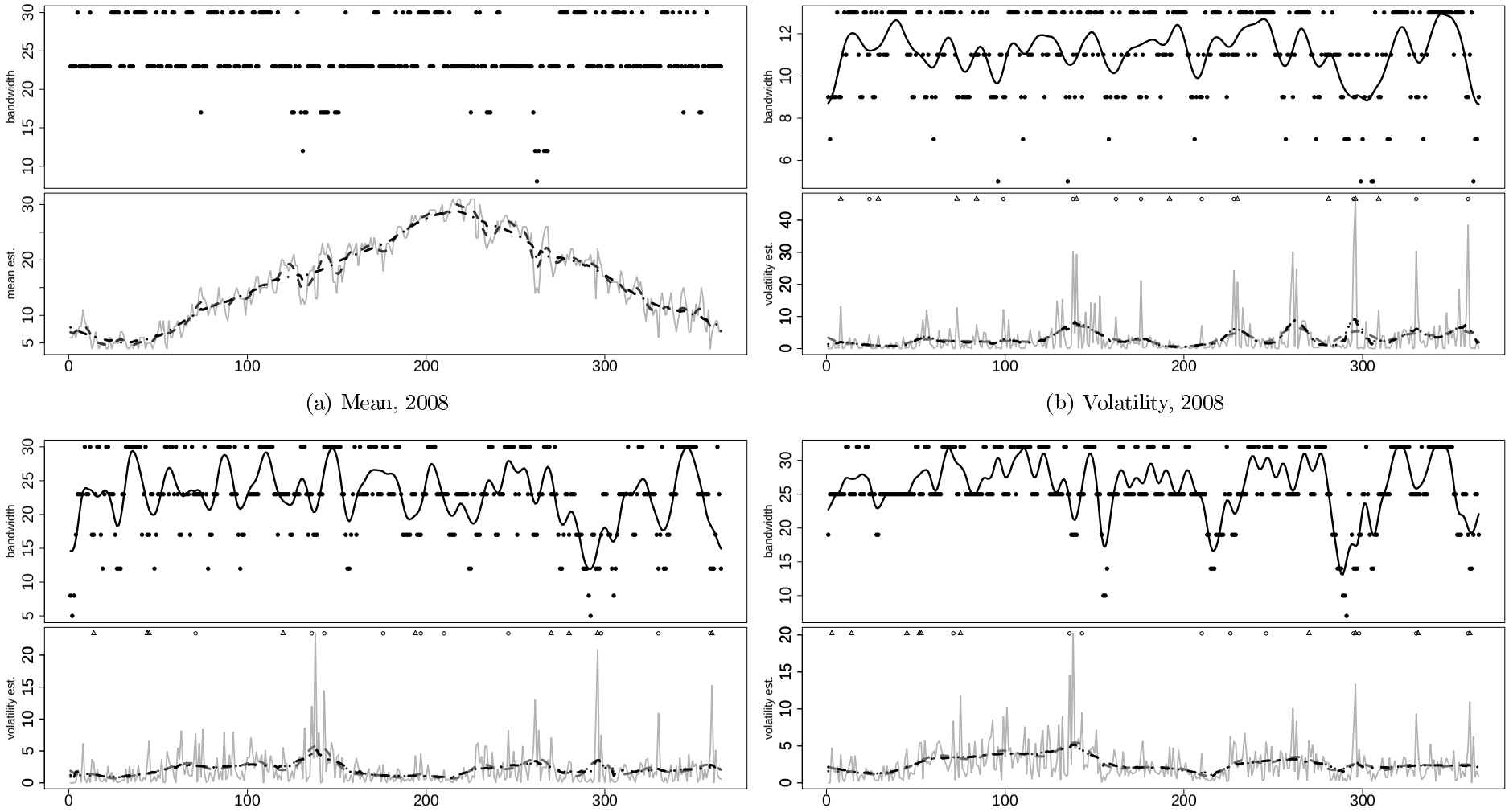


(a) Mean, 2008

(b) Volatility, 2008

(c) Volatility, 2006-2008

(d) Volatility, 2004-2008

Figure 9: Estimation of mean and variance for Tokyo. In each figure sequence (also smoothed for volatility) of bandwidths (upper panel), nonparametric function estimation (solid grey line), with fixed bandwidth (dashed line), adaptive bandwidth (dot-dashed line) and smoothed adaptive bandwidth (dotted line) (bottom panel of each figure).

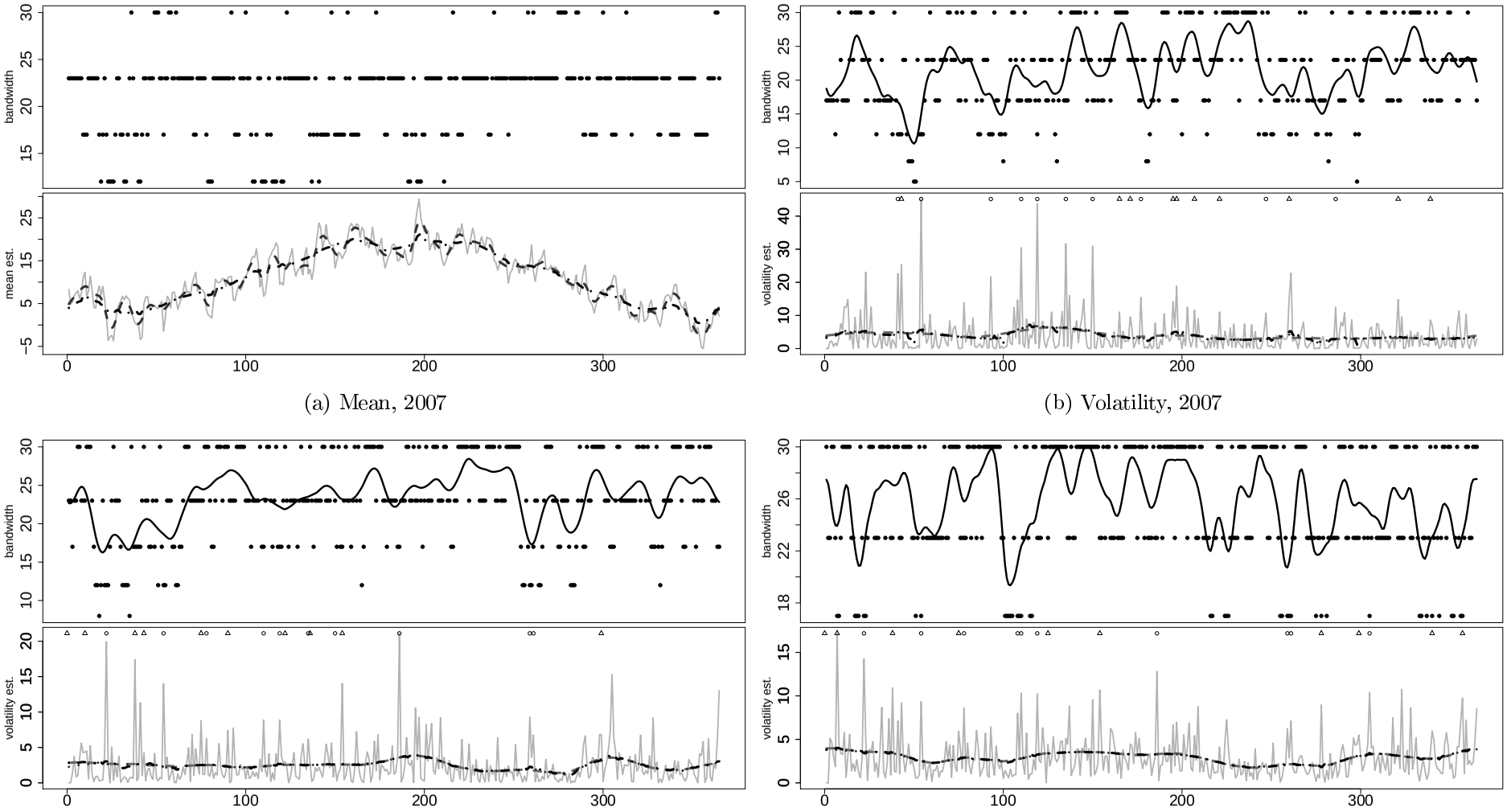


(a) Mean, 2007

(b) Volatility, 2007

(c) Volatility, 2005-2007

(d) Volatility, 2003-2007

Figure 10: Estimation of mean and variance for Berlin. In each figure sequence (also smoothed for volatility) of bandwidths (upper panel), nonparametric function estimation (solid grey line), with fixed bandwidth (dashed line), adaptive bandwidth (dot-dashed line) and smoothed adaptive bandwidth (dotted line) (bottom panel of each figure).

An approach to cope with the non normality brought in by more observations is to estimate mean functions year by year (SeMe), and then aggregate the residuals for variance estimation. We therefore estimate the joint/separate seasonal mean (JoMe/SeMe) and seasonal variance (Vo) curves with fixed bandwidth curve (fi), adaptive bandwidth curve (ad) and adaptive smoothed bandwidth (ads). Table 5 and Table 6 show the $p$-values for normality tests. Volatility plots on the Figures 7-10 displays the behavior of the variance function estimation when the period length changes. The average over years acts as a smoother when we consider more years. The estimated $AR(L)$ parameters for different cities using joint/separate mean (JoMe/SeMe) with different bandwidth curves are illustrated in Table 4. The results again show that an $AR(3)$ fits well the stylised facts of temperature.

The $p$-values of normality test statistics (Kolmogorov Smirnov KS, Jarques-Bera JB, Anderson Darling AD) of corrected residuals (after seasonal mean and volatility) for different cities under varying localising schemes are displayed in Table 5 and Table 6. The results are compared for different periods (3 years, 4 years, 5 years). The longer the period, the smaller the $p$-value of normality and therefore the more likely to reject the normality assumption. The standardised residuals are closer to normality (Berlin and New York) or at the same level (Kaoshiung and Tokyo) overall. The approach shows stability over more years. The $p$-values for adaptive estimates, over all cities, are generally larger than those for fixed bandwidth estimates. We observe that in US cities the risk factor show a better Gaussian pattern compared to other cities. With smoothed bandwidth, there are a slightly improvements in some cases. In most of the cases, specially in cities at sea level, the correction by adaptive models outperforms the classical method.

We tackle the problem of loosing information when considering estimates at individual level or averaging mean functions over time, with a refined approach that considers the minimum variance between the aggregation of yearly local mean function estimates and an optimal local estimate $\theta^o$. Once the sets of local mean functions have been identified, the aggregated local function can be defined as the weighted average of all the observations in a given time set. Formally, if $\hat{\theta}^j(t)$ is the localised observation at time $t$ of year $j$, the aggregated local function is given by:

$$\hat{\theta}_\omega(t) = \sum_{j=1}^{J} \omega_j \hat{\theta}^j(t). \tag{15}$$

With this aggregation step across $J$, we give the same weight to all observations, even to observations that were unimportant at the yearly level. Then a reasonable optimised estimate will be:

$$\arg\min_{\omega} \sum_{j=1}^{J} \sum_{t=1}^{365} \{\hat{\theta}_\omega(t) - \hat{\theta}_j^o(t)\}^2 \quad \text{subject to} \quad \sum_{j=1}^{J} \omega_j = 1; \omega_j > 0, j = 1, \ldots, J, \tag{16}$$

where the weights are assumed to be exogenous and nonstochastic, and $\hat{\theta}_j^o$ is defined as one of the following: 1 (SeMe Locave), $\hat{\theta}_j^o(t) = J^{-1} \sum_{j=1}^{J} \hat{\sigma}_j^2(t)$, the average of seasonal empirical variances over years, 2, (SeMe Locsep) $\hat{\theta}_j^o(t) = \hat{\sigma}_j^2(t)$, the yearly empirical variances, 3, one of above two approaches with maximised $p$-values over year. One may interpret this normalisation of weights as an optimisation with respect to different frequencies (yearly, daily). Table 5 and Table 6 display the results of the aggregation over time (Locave, Locsep, Locmax). Although the $p$-values decrease when considering more years, the aggregation approach performs drastically better than other approaches, especially in New York, because it weights more to extreme cases.

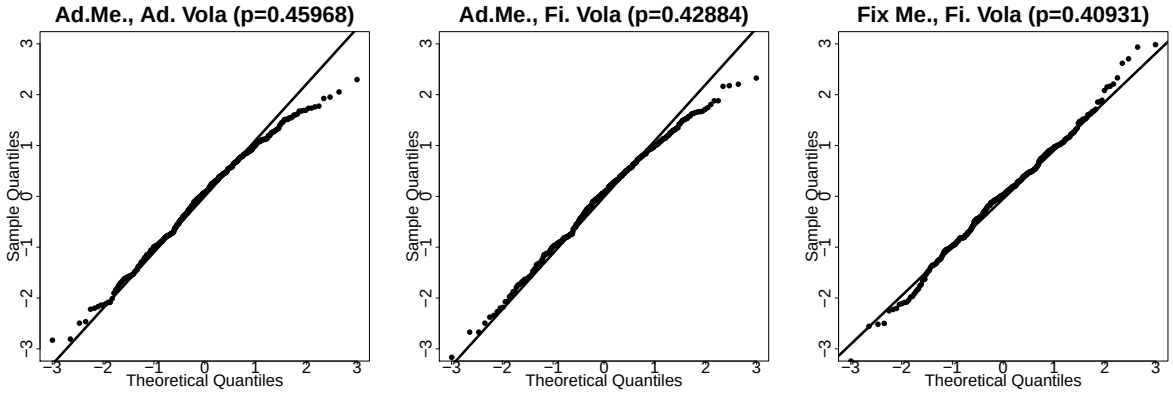


(a) Berlin 1 year (2007)

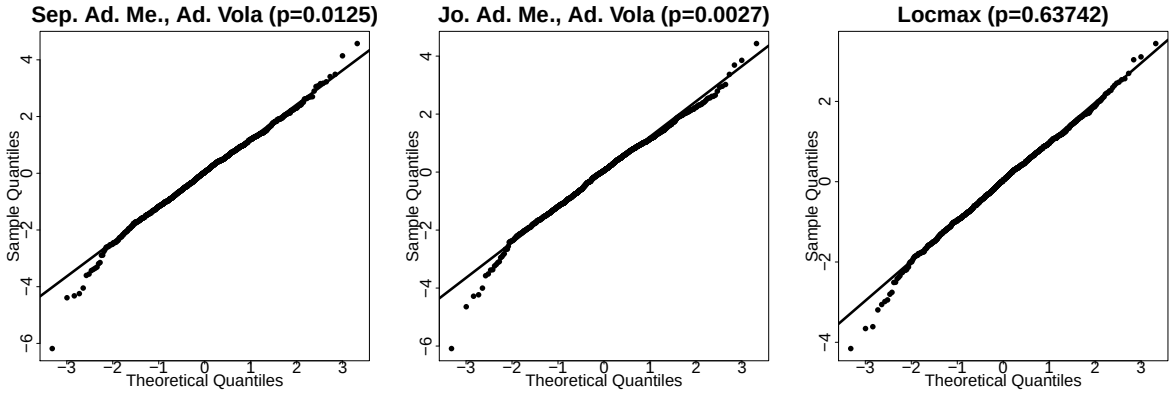


(b) Berlin 3 years (2004-2007)

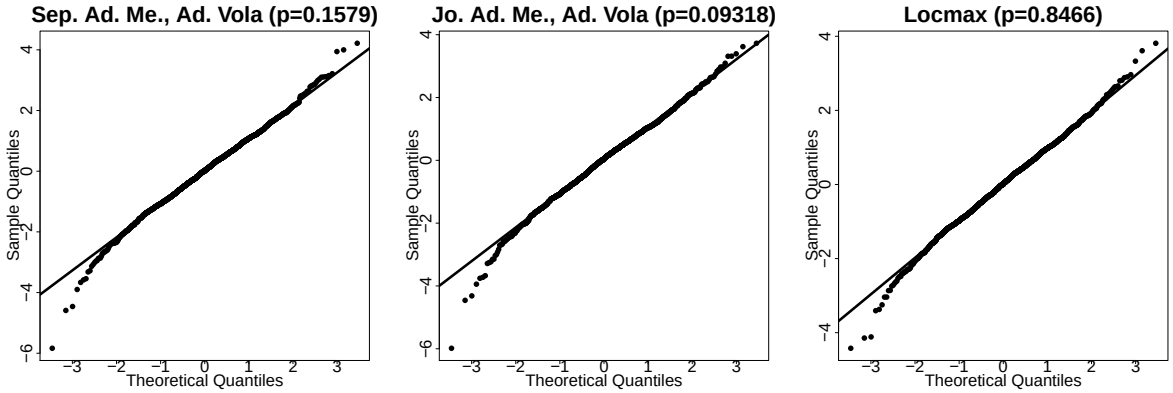


(c) Berlin 5 years (2002-2007)

Figure 11: QQ-plot for standardised residuals from Berlin using different methods.

| City | Method | Period | Mean | $\alpha_1$ | $\alpha_2$ | $\alpha_3$ | mean (AR) |
|---|---|---|---|---|---|---|---|
| Berlin | JoMe | 5 years | ad | 0.9719 | -0.2777 | 0.0971 | 0.0021 |
| | | | fi | 0.9607 | -0.2791 | 0.1092 | -1.1e-15 |
| | SeMe | 1 year | ad | 0.7131 | 0.1849 | - | 0.0346 |
| | | | fi | 0.1434 | -0.3480 | -0.1722 | -9.3e-16 |
| | | 2 years | ad | 0.8248 | -0.2435 | - | -0.0213 |
| | | | fi | 0.3267 | -0.3397 | -0.1390 | -9.7e-16 |
| | | 3 years | ad | 0.9120 | -0.2950 | - | -0.0054 |
| | | | fi | 0.3935 | -0.3418 | -0.1266 | -1.2e-16 |
| | | 4 years | ad | 0.8242 | -0.2823 | - | -0.0070 |
| | | | fi | 0.3091 | -0.3294 | -0.2674 | -9.6e-16 |
| | | 5 years | ad | 0.8217 | -0.2468 | - | -0.0006 |
| | | | fi | 0.3949 | -0.3491 | -0.1301 | -1.0e-15 |
| Tokyo | JoMe | 5 years | ad | 0.5869 | -0.0841 | 0.0340 | 7.0e-05 |
| | | | fi | 0.5820 | -0.0861 | 0.0348 | -2.2e-16 |
| | SeMe | 1 year | ad | 0.5093 | -0.1284 | - | 0.0093 |
| | | | fi | 0.2894 | -0.2213 | -0.1281 | -1.4e-15 |
| | | 2 years | ad | 0.4963 | -0.2146 | - | -0.0045 |
| | | | fi | 0.3744 | -0.3110 | - | -1.3e-15 |
| | | 3 years | ad | 0.4970 | -0.1475 | -0.0774 | 0.0112 |
| | | | fi | 0.3025 | -0.2194 | -0.1857 | -1.7e-15 |
| | | 4 years | ad | 0.3927 | -0.0244 | -0.1476 | -0.0035 |
| | | | fi | 0.1510 | -0.1538 | -0.2985 | -3.5e-16 |
| | | 5 years | ad | 0.5474 | -0.0663 | -0.0767 | 0.0298 |
| | | | fi | 0.2376 | -0.1828 | -0.2062 | -6.9e-16 |
| NewYork | JoMe | 5 years | ad | 0.7400 | -0.2250 | 0.1333 | -0.0016 |
| | | | fi | 0.7231 | -0.2288 | 0.1480 | -3.6e-16 |
| | SeMe | 1 year | ad | 0.6355 | -0.2447 | 0.1132 | 0.0068 |
| | | | fi | 0.3428 | -0.3384 | -0.0847 | -4.9e-17 |
| | | 2 years | ad | 0.4617 | -0.3050 | - | -0.0004 |
| | | | fi | 0.2983 | -0.3379 | -0.1517 | -2.2e-16 |
| | | 3 years | ad | 0.5154 | -0.2506 | - | 0.0007 |
| | | | fi | 0.1866 | -0.3466 | -0.1400 | 2.8e-16 |
| | | 4 years | ad | 0.6523 | -0.1757 | - | -0.0111 |
| | | | fi | 0.3440 | -0.2773 | -0.1181 | 4.9e-16 |
| | | 5 years | ad | 0.6761 | -0.2225 | - | 0.0168 |
| | | | fi | 0.5069 | -0.2846 | -0.0768 | -3.5e-16 |
| Kaohsiung | JoMe | 5 years | ad | 0.7969 | -0.1341 | - | 0.0027 |
| | | | fi | 0.7801 | -0.1205 | - | -1.9e-15 |
| | SeMe | 1 year | ad | 0.4292 | - | - | 0.0155 |
| | | | fi | 0.2695 | -0.1103 | -0.0792 | 1.1e-15 |
| | | 2 years | ad | 0.7388 | -0.2736 | -0.0752 | 0.0526 |
| | | | fi | 0.4569 | -0.3257 | -0.2248 | -6.1e-16 |
| | | 3 years | ad | 0.5482 | -0.0936 | -0.1875 | 0.0291 |
| | | | fi | 0.4783 | -0.1585 | -0.2173 | -6.7e-16 |
| | | 4 years | ad | 0.5625 | -0.1269 | -0.1556 | 0.0210 |
| | | | fi | 0.4719 | -0.1740 | -0.2126 | 6.2e-16 |
| | | 5 years | ad | 0.6219 | -0.1742 | - | 0.0284 |
| | | | fi | 0.4097 | -0.2231 | -0.0981 | 2.9e-16 |

Table 4: $AR(L)$ parameters for Berlin (20020101-20071201), Tokyo (20030101-20081201), New-York (20030101-20081201) and Kaohsiung (20030101-20081201) using joint/separate mean (JoMe/SeMe) with fixed bandwidth curve (fi), adaptive bandwidth curve (ad), adaptive smoothed bandwidth (ads) seasonal mean/volatility (Me/Vo) curve.

| | Method | p-Values (1 year) | | | p-Values (2 years) | | | p-Values (3 years) | | | p-Values (4 years) | | | p-Values (5 years) | | |
|---|---|---|---|---|---|---|---|---|---|---|---|---|---|---|---|---|
| | | KS | JB | AD | KS | JB | AD | KS | JB | AD | KS | JB | AD | KS | JB | AD |
| Berlin | JoMe adMe fiVo | 0.4288 | 0.0387 | 0.0215 | 4.7e-05 | 2.2e-08 | 0.0111 | 0.0037 | 0.0000 | 0.0032 | 0.0963 | 4.4e-15 | 0.0164 | 0.0797 | 1.1e-16 | 0.0005 |
| | JoMe adMe adVo | 0.4596 | 0.0185 | 0.0076 | 5.0e-05 | 4.6e-05 | 0.0214 | 0.0026 | 3.2e-11 | 0.0050 | 0.0919 | 1.3e-14 | 0.0201 | 0.0931 | 1.1e-16 | 0.0007 |
| | JoMe adMe adsVo | 0.4818 | 0.0185 | 0.0076 | 5.1e-05 | 4.6e-05 | 0.0214 | 0.0029 | 3.2e-11 | 0.0051 | 0.0824 | 1.3e-14 | 0.0201 | 0.0823 | 1.1e-16 | 0.0007 |
| | JoMe fiMe fiVo | 0.4093 | 0.3974 | 0.1171 | 3.0e-05 | 2.8e-05 | 0.0467 | 0.0041 | 2.6e-13 | 0.0007 | 0.1165 | 4.4e-11 | 0.0094 | 0.0952 | 1.2e-15 | 0.0004 |
| | JoMe fiMe adVo | 0.7194 | 0.1951 | 0.3372 | 4.0e-05 | 0.0296 | 0.0766 | 0.0039 | 1.1e-08 | 0.0010 | 0.1215 | 1.0e-09 | 0.0113 | 0.0967 | 1.1e-15 | 0.0005 |
| | JoMe fiMe adsVo | 0.6430 | 0.1951 | 0.3372 | 2.9e-05 | 0.0296 | 0.0766 | 0.0051 | 1.1e-08 | 0.0010 | 0.1237 | 1.0e-09 | 0.0113 | 0.0990 | 1.1e-15 | 0.0005 |
| | SeMe adMe fiVo | | | | 4.1e-05 | 8.3e-08 | 0.0758 | 0.0123 | 5.4e-15 | 0.0232 | 0.0387 | 1.1e-14 | 0.0259 | 0.1416 | 9.3e-13 | 0.0189 |
| | SeMe adaMe adVo | | | | 6.9e-05 | 0.0002 | 0.3148 | 0.0124 | 1.0e-10 | 0.0531 | 0.0429 | 8.8e-16 | 0.0284 | 0.1578 | 2.6e-14 | 0.0178 |
| | SeMe adaMe adsVo | | | | 2.8e-05 | 0.0002 | 0.3148 | 0.0105 | 1.0e-10 | 0.0531 | 0.0507 | 8.8e-16 | 0.0284 | 0.1511 | 2.6e-14 | 0.0178 |
| | SeMe fiMe fiVo | | | | 0.0005 | 0.0003 | 0.0028 | 0.0224 | 2.4e-05 | 0.0103 | 0.1206 | 1.5e-06 | 0.0037 | 0.2686 | 4.8e-06 | 0.0013 |
| | SeMe fiMe adVo | | | | 0.0001 | 0.0160 | 0.0165 | 0.0250 | 0.0015 | 0.0274 | 0.1317 | 7.3e-06 | 0.0064 | 0.3197 | 8.9e-07 | 0.0017 |
| | SeMe fiMe adsVo | | | | 0.0001 | 0.0160 | 0.0165 | 0.0239 | 0.0015 | 0.0274 | 0.1126 | 7.3e-06 | 0.0064 | 0.2050 | 8.9e-07 | 0.0017 |
| | SeMe Locave | | | | 0.7775 | 0.0413 | 0.3250 | 0.5355 | 0.0005 | 0.1515 | 0.7189 | 4.1e-06 | 0.1123 | 0.7566 | 1.0e-06 | 0.0504 |
| | SeMe Locsep | | | | 0.7775 | 0.0413 | 0.3250 | 0.5355 | 0.0005 | 0.1515 | 0.7191 | 4.1e-06 | 0.1125 | 0.7801 | 9.3e-07 | 0.0532 |
| | SeMe Locmax | | | | 0.8304 | 0.0919 | 0.2946 | 0.6374 | 0.0001 | 0.1329 | 0.7522 | 9.1e-07 | 0.0874 | 0.8465 | 4.8e-08 | 0.0400 |
| Kaohsiung | JoMe adMe fiVo | 0.0533 | 7.9e-07 | 2.4e-06 | 9.7e-06 | 7.1e-14 | 4.6e-10 | 0.0015 | 0.0000 | 9.9e-16 | 0.0003 | 0.0000 | 1.8e-21 | 9.7e-05 | 0.0000 | 2.1e-25 |
| | JoMe adMe adVo | 0.0540 | 8.3e-05 | 7.1e-06 | 4.7e-06 | 4.7e-13 | 3.48e-09 | 0.0015 | 0.0000 | 5.3e-15 | 0.0003 | 0.0000 | 2.1e-21 | 0.0012 | 0.0000 | 3.2e-25 |
| | JoMe adMe adsVo | 0.0543 | 8.3e-05 | 7.1e-06 | 3.8e-06 | 4.6e-13 | 3.48e-09 | 0.0013 | 0.0000 | 5.3e-15 | 0.0003 | 0.0000 | 2.1e-21 | 0.0001 | 0.0000 | 3.2e-25 |
| | JoMe fiMe fiVo | 0.2098 | 0.0020 | 0.0004 | 0.0001 | 2.1e-11 | 1.9e-08 | 0.0024 | 0.0000 | 3.2e-15 | 0.0004 | 0.0000 | 5.9e-21 | 9.3e-05 | 0.0000 | 3.9e-25 |
| | JoMe fiMe adVo | 0.2208 | 0.0092 | 0.0008 | 5.36e-05 | 9.6e-13 | 9.9e-08 | 0.0020 | 0.0000 | 1.9e-14 | 0.0005 | 0.0000 | 3.2e-20 | 0.0001 | 0.0000 | 1.6e-24 |
| | JoMe fiMe adsVo | 0.2269 | 0.0092 | 0.0008 | 6.99e-05 | 9.6e-13 | 9.9e-08 | 0.0025 | 0.0000 | 1.9e-14 | 0.0006 | 0.0000 | 3.2e-20 | 0.0001 | 0.0000 | 1.6e-24 |
| | SeMe adMe fiVo | | | | 2.1e-09 | 1.0e-14 | 4.3e-10 | 6.4e-05 | 0.0000 | 2.8e-12 | 0.0015 | 0.0000 | 2.2e-14 | 0.0019 | 0.0000 | 8.6e-18 |
| | SeMe adMe adVo | | | | 5.1e-09 | 0.0000 | 2.5e-08 | 5.1e-05 | 0.0000 | 1.0e-11 | 0.0016 | 0.0000 | 3.5e-14 | 0.0020 | 0.0000 | 1.4e-17 |
| | SeMe adMe adsVo | | | | 1.2e-08 | 0.0000 | 2.5e-08 | 4.9e-05 | 0.0000 | 1.0e-11 | 0.0014 | 0.0000 | 3.5e-14 | 0.0018 | 0.0000 | 1.4e-17 |
| | SeMe fiMe fiVo | | | | 3.0e-07 | 8.5e-09 | 3.8e-07 | 0.0004 | 4.9e-12 | 1.6e-08 | 0.0081 | 1.1e-12 | 4.0e-10 | 0.0084 | 0.0000 | 2.7e-13 |
| | SeMe fiMe adVo | | | | 5.8e-08 | 9.6e-14 | 1.6e-05 | 0.0004 | 1.5e-10 | 8.5e-08 | 0.0068 | 3.0e-12 | 7.3e-10 | 0.0080 | 0.0000 | 2.1e-13 |
| | SeMe fiMe adsVo | | | | 1.9e-07 | 9.6e-14 | 1.6e-05 | 0.0004 | 1.5e-10 | 8.5e-08 | 0.0078 | 3.0e-12 | 7.3e-10 | 0.0075 | 0.0000 | 2.1e-13 |
| | SeMe Locave | | | | 0.0165 | 1.6e-08 | 3.0e-09 | 0.0131 | 1.1e-14 | 1.8e-11 | 0.0046 | 0.0000 | 1.1e-13 | 0.0004 | 0.0000 | 1.0e-16 |
| | SeMe Locsep | | | | 0.0165 | 1.6e-08 | 3.0e-09 | 0.0131 | 1.1e-14 | 1.8e-11 | 0.0046 | 0.0000 | 1.1e-13 | 0.0003 | 0.0000 | 1.0e-16 |
| | SeMe Locmax | | | | 0.0302 | 1.5e-08 | 2.9e-09 | 0.0163 | 6.7e-15 | 1.1e-11 | 0.0061 | 0.0000 | 9.8e-14 | 0.0046 | 0.0000 | 9.2e-17 |

Table 5: $p$-values of Jarque Bera (JB), Kolmogorov Smirnov (KS) and Anderson Darling (AD) test statistics for Berlin (20020101-20071201) & Kaohsiung (20020101-20071201) corrected residuals under different adaptive localising schemes: for joint/separate mean (JoMe/SeMe) with fixed bandwidth curve (fi), adaptive bandwidth curve (ad), adaptive smoothed bandwidth (ads) seasonal mean/volatility (Me/Vo) curve.

# 4 A temperature pricing example

Futures and options written on temperature indices are traded at the Chicago Mercantile Exchange (CME). Temperature futures are contracts written on different temperature indices measured over specified periods $[\tau_1, \tau_2]$ like weeks, months or quarters of a year. The owner of a call option written on futures $F_{(t,\tau_1,\tau_2)}$ with exercise time $t \leq \tau_1$ and measurement period $[\tau_1, \tau_2]$ will receive $\max\left\{F_{(t,\tau_1,\tau_2)} - K, 0\right\}$. The most common temperature indices are: Heating Degree Day (HDD), Cooling Degree Day (CDD), Cumulative Averages (CAT) (or Average Acumulative Temperatures AAT). The CAT index accounts the accumulated average temperature over $[\tau_1, \tau_2]$:

$$CAT(\tau_1, \tau_2) = \int_{\tau_1}^{\tau_2} T_u du,$$

where $T_u = (T_{u,max} + T_{u,min})/2$ and the measurement period is usually a month or season. The HDD index measures the cumulative amount of average temperature below a threshold (typically 18°C or 65°F) over a period $[\tau_1, \tau_2]$: $\max(c - T_u, 0)$. Similarly, the CDD index accumulate $\max(T_u - c, 0)$. At CME, CAT-CDD futures are traded for European cities, CDD-HDD for US, Canada and Australian cities and AAT for Japanese cities.

Under the non-arbitrage pricing setting, a CAT temperature future is defined as:

$$F_{(t,\tau_1,\tau_2)} = \mathsf{E}^{Q_\lambda}\left[CAT(\tau_1, \tau_2)|\mathcal{F}_t\right],$$

where $\lambda$ denotes the market price of risk and the stochastic process for the daily average temperatures after removing seasonality ($X_t = T_t - \Lambda_t$) is assumed to follow a continuous-time autoregressive process $AR(L)(CAR(L))$ with deterministic seasonal variation $\sigma_t > 0$:

$$d\mathbf{X}_t = \mathbf{A}\mathbf{X}_t dt + \mathbf{e}_L \sigma_t dB_t, \tag{17}$$

where $\mathbf{X}_t \in \mathbb{R}^L$ for $L \geq 1$ denotes a vectorial Ornstein-Uhlenbeck process, $\mathbf{e}_k$ a $k$'th unit vector in $\mathbb{R}^L$ for $k = 1, ...L$, $B_t$ a Brownian motion and a $L \times L$-matrix $\mathbf{A}$:

$$\mathbf{A} = \begin{pmatrix} 0 & 1 & 0 & \dots & 0 & 0 \\ 0 & 0 & 1 & \dots & 0 & 0 \\ \vdots & & \ddots & & 0 & \vdots \\ 0 & \dots & \dots & 0 & 0 & 1 \\ -\alpha_L & -\alpha_{L-1} & \dots & & 0 & -\alpha_1 \end{pmatrix}$$

with positive constants $\alpha_k$. The $AR(L)$'s process estimated in (5) can be therefore seen as a discretely sampled continuous-time processes $(CAR(L))$ (17), see Härdle and López Cabrera (2010) or Benth et al. (2007) for more details. The last three columns of Table 1 display the $CAR(3)$-parameters for all temperature data. Then, for $0 \leq t \leq \tau_1 < \tau_2$, the explicit form of an $CAT$ future price is given by:

$$\begin{aligned} F_{CAT(t,\tau_1,\tau_2)} &= \mathsf{E}^{Q_\lambda}\left[\int_{\tau_1}^{\tau_2} T_u du|\mathcal{F}_t\right] \\ &= \int_{\tau_1}^{\tau_2} \Lambda_u du + \mathbf{a}_{t,\tau_1,\tau_2}\mathbf{X}_t + \int_t^{\tau_1} \lambda_u \sigma_u \mathbf{a}_{t,\tau_1,\tau_2}\mathbf{e}_L du \\ &+ \int_{\tau_1}^{\tau_2} \lambda_u \sigma_u \mathbf{e}_1^\top \mathbf{A}^{-1}\left[\exp\left\{\mathbf{A}(\tau_2 - u)\right\} - I_L\right]\mathbf{e}_L du \end{aligned} \tag{18}$$

with $\mathbf{a}_{t,\tau_1,\tau_2} = \mathbf{e}_1^\top \mathbf{A}^{-1} [\exp\{\mathbf{A}(\tau_2 - t)\} - \exp\{\mathbf{A}(\tau_1 - t)\}]$, $I_L$ a $L \times L$ identity matrix (Note that $\lambda_t \neq \Lambda_t$).

The options at CME are cash settled i.e. the owner of a future receives 20 times the Degree Day Index at the end of the measurement period, in return for a fixed price. At time $t$, CME trades different contracts $i = 1, \cdots, I$ with measurement period $t \leq \tau_1^i < \tau_2^i$. For example, a contract with $i = 7$ is six months ahead from the trading day $t$. For US and Europe CAT/CDD/HDD futures $I$ is usually equal to 7 (April-November or November-April), while for Asia $I = 12$ (Jan-Dec).

In order to achieve Gaussian risk factors and being able to price temperature future prices, we estimate $\Lambda_t$ and $\sigma_t$ by means of the previous adaptive smoothing techniques. The temperature prices given by CME, the index values computed from the realised temperature data $I_{(\tau_1,\tau_2)}$ and the estimated CAT-AAT future prices with separate adaptive bandwidth for seasonality in mean and volatility (SeMe Locave, SeMe Locsep, SeMe Locmax) of Berlin, Tokyo and Kaohsiung contracts are given in Table 7. By inverting (18), we inferred the MPR ($\lambda_t$) from traded weather futures in Berlin and Tokyo. As we see in Figure 12, the market price of risk for these products is different for different cities and contract types and time-varing but constant over contracts. We use the inferred MPR from Tokyo AAT futures to price over the counter (OTC) ATT futures for Kaohsiung. Similar to Härdle and López Cabrera (2010), we regress the average MPR of contract $i$ over the trading period, against the variation in period $[\tau_1, \tau_2]$, i.e.

$$\hat{\theta}^i_{\tau_1,\tau_2} = \frac{1}{\tau_1 - t} \sum_t^{\tau_1} \hat{\theta}^i_t,$$

$$\hat{\sigma}^2_{\tau_1,\tau_2} = \frac{1}{\tau_2 - \tau_1} \sum_{t=\tau_1}^{\tau_2} \hat{\sigma}^2_t.$$

The specification of the MPR is estimated as a deterministic function of volatility:

$$\lambda_t = 4.08 - 2.19\hat{\sigma}^2_{\tau_1,\tau_2} + 0.28\hat{\sigma}^4_{\tau_1,\tau_2}.$$

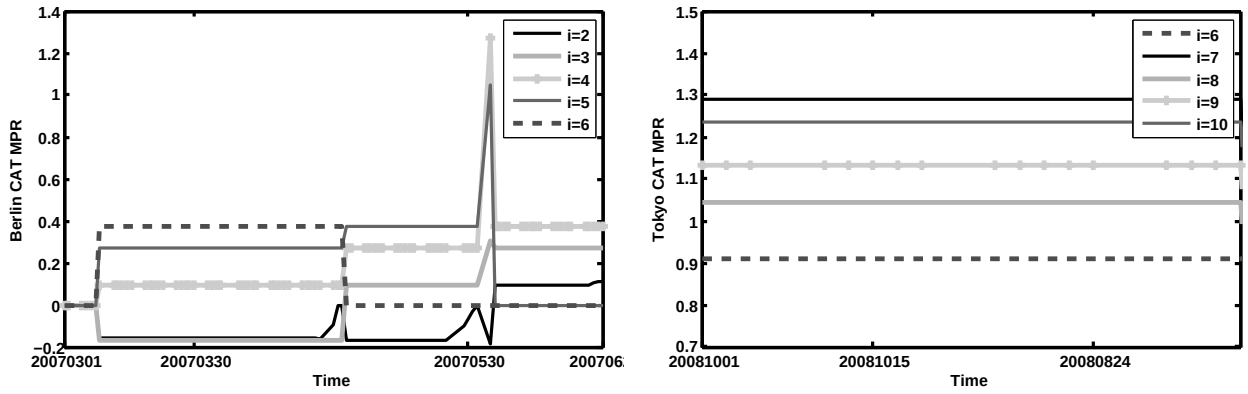


Figure 12: MPR for Berlin CAT futures and Tokyo AAT futures traded before measurement period.

A more general descriptive measure between the difference of CME and estimated prices is given

by root mean squared errors $RMSE's$:

$$RMSE = \sqrt{n^{-1}\sum_{i=1}^{n}(\hat{F}_{i,t,\tau_1,\tau_2} - I_{(\tau_1,\tau_2)})^2},$$

where $\hat{F}_{i,t,\tau_1,\tau_2}(i = 1, \ldots, n$ the number of contracts) are the estimates of future prices, and $I_{(\tau_1,\tau_2)}$ is the realised temperature in $[\tau_1, \tau_2]$. Table 8 shows the corresponding $RMSE's$. The results show smaller $RMSE's$ when future prices are estimated via pricing methods that consider an unbiased market price of weather risks. By using adaptive local methods, the estimates are closer to the market temperature prices, meaning that they have learned the market conditional of past weather surprises. This brings, of course, investment chances: someone who purchased a CAT contract for Berlin on 20070427 with $\tau_1 = 20070501$ and $\tau_2 = 20070531$ would have paid 9 140 EUR (1 index point = 20 EUR per contract, see Table 7 ). If he had held until expiration, a payoff 744 EUR (9 884-9 140 EUR) would had resulted. The last column of Table 7 shows the difference between CME prices (column 5) and the estimated risk neutral prices ($P = Q$ or $\lambda_t = 0$). Since the risk neutral prices are quite close to the realised temperature, they can act as a personal forecast for an investor. When the difference is positive, the strategy to hedge would be to buy a Call(C), and a Put(P) for negative difference. For example, if a farmer in Kaoshiung would like to hedge the exposure to weather risk, let us say that an accumulated average temperature of 825.89 index points during April 2009, one builds a portfolio of combinations of traded temperature derivatives e.g. Tokyo's contracts to replicate his payoff. In other words, the realised temperature in April $825.89(\text{C}) = 1 \times 118.32(\text{C}) + 1 \times 283.18(\text{C}) + 0.830395 \times 511.07(\text{C})$, where 118.32, 283.18 and 511.07 denote the CME AAT prices for April, May and June respectively.

# 5 Conclusions and further work

We show that temperature risk stochastics are closer to Gaussian when applying adaptive statistical methods. We demonstrate that a local smoothing procedure corrects for seasonality and volatility. Technically, the proposed adaptive technique is rooted in ideas of Mercurio and Spokoiny (2004); Spokoiny (2009). We found that the method performs well, not mattering the specification given for $\Lambda_t$ or $\sigma_t$.

The localisation works by selection of weights (at each time point $t$) from a finite number of localising schemes $W^k, k = 1, \ldots, K$. We calculate local parametric MLEs $\tilde{\theta}_k$ that satisfy a small modeling bias condition. The adaptation of parameters increases the procedures's flexibility and estimation accuracy. We also observed in most of the cases, that the proposed method outperforms the standard estimation methods. One obtains fair temperature derivative prices and consequently an unbiased market price of weather risk.

# References

Benth, F., Benth, S. and Koekebakker, S. (2007). Putting a price on temperature., *Scandinavian Journal of Statistics* **34**: 746–767.

Benth, F., Härdle, W. K. and López Cabrera, B. (2011). *Pricing Asian temperature risk in Statistical Tools for Finance and Insurance 2nd. edition (Cizek, Härdle and Weron, eds.)*, Springer Verlag Heidelberg.

Campbell, S. and Diebold, F. (2005). Weather forecasting for weather derivatives, *Journal of American Statistical Association* **100(469)**: 6–16.

Chen, Y., Härdle, W. K. and Pigorsch, U. (2010). Localized realized volatility modelling, *Journal of the American Statistical Association, to appear* .

Cízek, P., Härdle, W. K. and Spokoiny, V. (2009). Adaptive pointwise estimation in time-inhomogeneous conditional heteroschedasticity models, *The Econometrics Journal* **12**: 248–271.

Diebold, F. and Inoue, A. (2001). Long memory and regime switching, *Journal of Econometrics* **105**: 131–159.

Granger, C. and Hyung, N. (2004). Occasional structural breaks and long memory with an application to the s&p 500 absolute stock returns, *Journal of Empirical Finance* **11**: 399–421.

Härdle, W. K. and López Cabrera, B. (2010). Infering the market price of weather risk, *Applied Mathematical Finance, invitation to be resubmitted, preprint is available as SFB 649 Discussion Paper under http://sfb649.wiwi.hu-berlin.de/papers/pdf/SFB649DP2009-001.pdf* .

Horst, U. and Mueller, M. (2007). On the spanning property of risk bonds priced by equilibrium, *Mathematics of Operation Research* **32(4)**: 784–807.

Karatzas, I. and Shreve, S. (2001). *Methods of Mathematical Finance.*, Springer Verlag, New York.

Mercurio, D. and Spokoiny, V. (2004). Statistical inference for time-inhomogeneous volatility models, *The Annals of Statistics* **32(2)**: 577–602.

Polzehl, J. and Spokoiny, V. (2006). Propagation-separation approach for local likelihood estimation, *Probability Theory and Realated Fields* **135**: 335–362.

Spokoiny, V. (2009). Multiscale local change point detection with applications to value at risk, *The Annals of Statistics* **37**(3): 1405–1436.

| | Method | p-Values (1 years) | | | p-Values (2 years) | | | p-Values (3 years) | | | p-Values (4 years) | | | p-Values (5 years) | | |
|---|---|---|---|---|---|---|---|---|---|---|---|---|---|---|---|---|
| | | KS | JB | AD | KS | JB | AD | KS | JB | AD | KS | JB | AD | KS | JB | AD |
| New-York | JoMe adMe fiVo | 0.8746 | 0.6556 | 0.5138 | 4.9e-05 | 0.3354 | 0.7356 | 0.0068 | 0.2725 | 0.3993 | 0.0089 | 0.0151 | 0.0402 | 0.0190 | 0.0208 | 0.0819 |
| | JoMe adMe adVo | 0.9912 | 0.1562 | 0.3016 | 1.7e-05 | 0.3515 | 0.7762 | 0.0200 | 0.1461 | 0.2937 | 0.0148 | 0.0031 | 0.0182 | 0.0284 | 0.0025 | 0.0107 |
| | JoMe adMe adsVo | 0.9749 | 0.1562 | 0.3016 | 2.3e-05 | 0.3515 | 0.7762 | 0.0256 | 0.1461 | 0.2937 | 0.0136 | 0.0031 | 0.0182 | 0.0391 | 0.0025 | 0.0107 |
| | JoMe fiMe fiVo | 0.9862 | 0.8166 | 0.7973 | 0.0001 | 0.4139 | 0.7380 | 0.0280 | 0.3182 | 0.2855 | 0.0246 | 0.0111 | 0.0239 | 0.0446 | 0.0207 | 0.0574 |
| | JoMe fiMe adVo | 0.9891 | 0.3916 | 0.5883 | 0.0002 | 0.3364 | 0.8056 | 0.0528 | 0.1957 | 0.2264 | 0.0816 | 0.0012 | 0.0077 | 0.0849 | 0.0031 | 0.0096 |
| | JoMe fiMe adsVo | 0.9870 | 0.3916 | 0.5883 | 0.0002 | 0.3364 | 0.8056 | 0.0592 | 0.1957 | 0.2264 | 0.0896 | 0.0012 | 0.0077 | 0.0923 | 0.0031 | 0.0096 |
| | SeMe adMe fiVo | | | | 2.0e-08 | 0.6712 | 0.2900 | 0.0004 | 0.9518 | 0.8551 | 0.0006 | 0.4751 | 0.4227 | 0.0030 | 0.4697 | 0.3803 |
| | SeMe adMe adVo | | | | 1.4e-08 | 0.6987 | 0.3244 | 0.0012 | 0.4515 | 0.5522 | 0.0020 | 0.1522 | 0.1491 | 0.0082 | 0.0733 | 0.1291 |
| | SeMe adMe adsVo | | | | 4.7e-08 | 0.6987 | 0.3244 | 0.0010 | 0.4515 | 0.5522 | 0.0022 | 0.1522 | 0.1491 | 0.0058 | 0.0730 | 0.1291 |
| | SeMe fiMe fiVo | | | | 9.7e-07 | 0.8913 | 0.1930 | 0.0004 | 0.5421 | 0.0614 | 0.0007 | 0.9999 | 0.0276 | 0.0029 | 0.5896 | 0.0086 |
| | SeMe fiMe adVo | | | | 8.7e-07 | 0.5614 | 0.1298 | 0.0012 | 0.5853 | 0.0574 | 0.0015 | 0.7922 | 0.0277 | 0.0090 | 0.3283 | 0.0082 |
| | SeMe fiMe adsVo | | | | 2.1e-06 | 0.5614 | 0.1298 | 0.0014 | 0.5853 | 0.0574 | 0.0019 | 0.7922 | 0.0277 | 0.0086 | 0.3283 | 0.0082 |
| | SeMe Locave | | | | 0.7457 | 0.2267 | 0.1804 | 0.7307 | 0.6553 | 0.7516 | 0.4735 | 0.2630 | 0.2108 | 0.6619 | 0.3046 | 0.2056 |
| | SeMe Locsep | | | | 0.7457 | 0.2267 | 0.1804 | 0.7305 | 0.6553 | 0.7515 | 0.4756 | 0.2631 | 0.2107 | 0.6623 | 0.3045 | 0.2056 |
| | SeMe Locmax | | | | 0.8456 | 0.2402 | 0.2053 | 0.9788 | 0.6824 | 0.7495 | 0.7526 | 0.2191 | 0.1788 | 0.7900 | 0.2418 | 0.1602 |
| Tokyo | JoMe adMe fiVo | 0.3299 | 0.1130 | 0.0229 | 0.0025 | 3.8e-09 | 1.3e-06 | 0.0270 | 1.4e-07 | 5.1e-05 | 0.2132 | 2.3e-09 | 1.4e-05 | 0.3138 | 2.6e-10 | 2.7e-06 |
| | JoMe adMe adVo | 0.5743 | 0.1327 | 0.0470 | 0.0013 | 2.6e-10 | 0.0006 | 0.0812 | 1.7e-06 | 0.0002 | 0.2588 | 1.0e-09 | 1.1e-05 | 0.2731 | 5.5e-10 | 1.9e-06 |
| | JoMe adMe adsVo | 0.5544 | 0.1327 | 0.0470 | 0.0006 | 2.6e-10 | 0.0006 | 0.0511 | 1.7e-06 | 0.0002 | 0.1995 | 1.0e-09 | 1.1e-05 | 0.1990 | 5.5e-10 | 1.9e-06 |
| | JoMe fiMe fiVo | 0.9588 | 0.3707 | 0.8936 | 0.0052 | 3.0e-08 | 5.7e-06 | 0.0647 | 1.7e-07 | 0.0001 | 0.2348 | 6.2e-11 | 7.1e-06 | 0.3211 | 4.7e-11 | 1.5e-06 |
| | JoMe fiMe adVo | 0.9809 | 0.1317 | 0.4861 | 0.0022 | 1.0e-08 | 0.0019 | 0.1032 | 4.1e-06 | 0.0004 | 0.2545 | 2.0e-10 | 9.5e-06 | 0.3127 | 8.4e-11 | 1.0e-06 |
| | JoMe fiMe adsVo | 0.9807 | 0.1317 | 0.4861 | 0.0012 | 1.0e-08 | 0.0019 | 0.0705 | 4.1e-06 | 0.0004 | 0.2488 | 2.0e-10 | 9.5e-06 | 0.2769 | 8.4e-11 | 1.0e-06 |
| | SeMe adMe fiVo | | | | 9.2e-05 | 7.2e-13 | 2.2e-05 | 0.0045 | 5.5e-10 | 0.0001 | 0.0693 | 4.5e-14 | 9.5e-06 | 0.2642 | 4.6e-13 | 1.0e-05 |
| | SeMe adMe adVo | | | | 2.3e-05 | 5.0e-07 | 0.0005 | 0.0471 | 5.6e-09 | 8.9e-05 | 0.1865 | 4.2e-13 | 1.0e-05 | 0.3357 | 7.6e-13 | 9.5e-06 |
| | SeMe adMe adsVo | | | | 6.8e-05 | 5.0e-07 | 0.0005 | 0.0315 | 5.6e-09 | 8.9e-05 | 0.1896 | 4.2e-13 | 1.0e-05 | 0.2821 | 7.6e-13 | 9.5e-06 |
| | SeMe fiMe fiVo | | | | 0.0002 | 1.8e-08 | 0.0002 | 0.0424 | 7.0e-08 | 4.8e-05 | 0.2124 | 5.5e-16 | 1.6e-06 | 0.3126 | 0.0000 | 1.4e-07 |
| | SeMe fiMe adVo | | | | 0.0001 | 2.7e-05 | 0.0025 | 0.0638 | 1.5e-07 | 9.0e-05 | 0.3012 | 3.1e-15 | 3.1e-06 | 0.3265 | 1.8e-11 | 1.3e-06 |
| | SeMe fiMe adsVo | | | | 9.7e-05 | 2.7e-05 | 0.0025 | 0.0545 | 1.5e-07 | 9.0e-05 | 0.2417 | 3.1e-15 | 3.1e-06 | 0.3220 | 1.8e-11 | 1.3e-06 |
| | SeMe Locave | | | | 0.1075 | 0.0271 | 0.0026 | 0.1065 | 0.0002 | 0.0006 | 0.0714 | 3.0e-06 | 0.0001 | 0.0620 | 9.2e-07 | 5.5e-05 |
| | SeMe Locsep | | | | 0.1075 | 0.0271 | 0.0026 | 0.1065 | 0.0002 | 0.0006 | 0.0714 | 3.0e-06 | 0.0001 | 0.0619 | 9.1e-07 | 5.5e-05 |
| | SeMe Locmax | | | | 0.4641 | 0.0269 | 0.0029 | 0.4898 | 0.0003 | 0.0009 | 0.5045 | 2.0e-06 | 0.0001 | 0.4086 | 3.1e-07 | 5.9e-05 |

Table 6: $p$-values of Jarque Bera (JB), Kolmogorov Smirnov (KS) and Anderson Darling (AD) test statistics for New-York (20030101-20081201) & Tokyo (20030101-20081201) corrected residuals under different adaptive localising schemes: for joint/separate mean (JoMe/SeMe) with fixed bandwidth curve (fi), adaptive bandwidth curve (ad), adaptive smoothed bandwidth (ads) seasonal mean/volatility (Me/Vo) curve.

| | Trading date | Measurement Period | | | Future Prices $F_{(t,\tau_1,\tau_2,\lambda_t,\hat{\theta})}$ | | | | Realised $T_t$ | |
|---|---|---|---|---|---|---|---|---|---|---|
| Contract type | $t$ | $\tau_1$ | $\tau_2$ | CME | $\lambda_t = 0$ | $\lambda_t = \lambda$ SeMe Locave | $\lambda_t = \lambda$ SeMe Locsep | $\lambda_t = \lambda$ SeMe Locmax | $I_{(\tau_1,\tau_2)}$ | Strategy |
| Berlin-CAT | 20070316 | 20070401 | 20070430 | 288.00 | 363.00 | 291.06 | 290.92 | 291.12 | 362.90 | -75.00(P) |
| Berlin-CAT | 20070316 | 20070501 | 20070531 | 457.00 | 502.11 | 454.91 | 454.22 | 455.38 | 494.20 | -45.00(P) |
| Berlin-CAT | 20070316 | 20070601 | 20070630 | 529.00 | 571.78 | 634.76 | 634.05 | 633.76 | 574.30 | -42.00(P) |
| Berlin-CAT | 20070316 | 20070701 | 20070731 | 616.00 | 591.56 | 686.76 | 683.69 | 684.31 | 583.00 | 25.00(C) |
| Berlin-CAT | 20070316 | 20070801 | 20070831 | 610.00 | 566.14 | 736.22 | 736.00 | 748.65 | 580.70 | 43.86(C) |
| Berlin-CAT | 20070316 | 20070901 | 20070930 | 472.00 | 414.33 | 472.00 | 472.00 | 472.00 | 414.80 | 57.67(C) |
| Berlin-CAT | 20070427 | 20070501 | 20070531 | 457.00 | 506.18 | 457.52 | 456.82 | 458.07 | 494.20 | -49.18(P) |
| Berlin-CAT | 20070427 | 20070601 | 20070630 | 529.00 | 571.78 | 634.76 | 634.05 | 633.76 | 574.30 | -42.78(P) |
| Berlin-CAT | 20070427 | 20070701 | 20070731 | 616.00 | 591.56 | 686.76 | 683.69 | 684.31 | 583.00 | 24.44(C) |
| Berlin-CAT | 20070427 | 20070801 | 20070831 | 610.00 | 566.14 | 736.22 | 736.91 | 748.65 | 580.70 | 43.86(C) |
| Berlin-CAT | 20070427 | 20070901 | 20070930 | 472.00 | 414.33 | 472.00 | 472.00 | 472.00 | 414.80 | 57.67(C) |
| Kaohsiung-AAT | 20081028 | 20090301 | 20090331 | - | 754.82 | 775.28 | 775.50 | 839.39 | 739.00 | |
| Kaohsiung-AAT | 20081028 | 20090401 | 20090430 | - | 825.89 | 946.02 | 945.95 | 967.13 | 767.00 | |
| Kaohsiung-AAT | 20081028 | 20090501 | 20090531 | - | 879.26 | 1052.97 | 1050.30 | 1038.65 | 852.00 | |
| Kaohsiung-AAT | 20081028 | 20090601 | 20090630 | - | 852.60 | 921.29 | 922.31 | 937.02 | 872.00 | |
| Kaohsiung-AAT | 20081028 | 20090701 | 20090731 | - | 898.74 | 1059.37 | 1058.46 | 1042.18 | 923.00 | |
| Kaohsiung-AAT | 20081128 | 20090301 | 20090331 | - | 754.82 | 1552.57 | 1677.93 | 918.41 | 739.00 | |
| Kaohsiung-AAT | 20081128 | 20090401 | 20090430 | - | 825.89 | 837.19 | 837.12 | 873.50 | 767.00 | |
| Kaohsiung-AAT | 20081128 | 20090501 | 20090531 | - | 879.26 | 970.09 | 969.69 | 984.12 | 852.00 | |
| Kaohsiung-AAT | 20081128 | 20090601 | 20090630 | - | 852.60 | 958.67 | 959.16 | 956.36 | 872.00 | |
| Kaohsiung-AAT | 20081128 | 20090701 | 20090731 | - | 898.74 | 999.97 | 999.77 | 1009.92 | 923.00 | |
| Kaohsiung-AAT | 20081128 | 20090801 | 20090831 | - | 898.46 | 1008.29 | 1008.66 | 1002.90 | 918.00 | |
| Tokyo-AAT | 20081027 | 20090301 | 20090331 | 450.00 | 118.32 | 588.90 | 588.90 | 567.39 | 305.00 | 332.00(C) |
| Tokyo-AAT | 20081027 | 20090401 | 20090430 | 592.00 | 283.18 | 533.27 | 533.26 | 554.19 | 479.00 | 309.00(C) |
| Tokyo-AAT | 20081027 | 20090501 | 20090531 | 682.00 | 511.07 | 696.31 | 696.32 | 684.99 | 623.00 | 171.00(C) |
| Tokyo-AAT | 20081027 | 20090601 | 20090630 | 818.00 | 628.24 | 835.50 | 835.51 | 843.42 | 679.00 | 190.00(C) |
| Tokyo-AAT | 20081027 | 20090701 | 20090731 | 855.00 | 731.30 | 706.14 | 706.14 | 704.71 | 812.00 | 124.00(C) |

Table 7: Weather futures listed on date (yyyymmdd) at CME (Source: Bloomberg) and $\hat{F}_{t,\tau_1,\tau_2,\lambda,\theta}$ estimated prices with MPR ($\lambda_t$) under different localisation schemes ($\hat{\theta}$ under SeMe Locave, SeMe Locsep, SeMe Locmax), P(Put), C(Call)

| Contract type | Measurement Period | | | RMSE between $F_{(t,\tau_1,\tau_2,\lambda_t,\hat{\theta})}$ and CME prices | | | | |
|---|---|---|---|---|---|---|---|---|
| | $\tau_1$ | $\tau_2$ | No. contracts | $\lambda_t = 0$ | $\lambda_t = \lambda$ SeMe Locave | $\lambda_t = \lambda$ SeMe Locsep | $\lambda_t = \lambda$ SeMe Locmax | $I_{(\tau_1,\tau_2)}$ |
| Berlin-CAT | 20050401 | 20050430 | 62 | 25.39 | 14.74 | 14.72 | 14.75 | 26.63 |
| Berlin-CAT | 20050501 | 20050531 | 83 | 29.17 | 29.41 | 29.49 | 29.46 | 15.70 |
| Berlin-CAT | 20050601 | 20050630 | 104 | 8.02 | 89.97 | 88.93 | 88.39 | 8.65 |
| Berlin-CAT | 20050701 | 20050731 | 126 | 10.26 | 53.58 | 52.95 | 52.79 | 11.93 |
| Berlin-CAT | 20050801 | 20050831 | 146 | 68.88 | 77.03 | 76.95 | 77.59 | 85.95 |
| Berlin-CAT | 20050901 | 20050930 | 169 | 38.54 | 27.16 | 27.07 | 27.22 | 43.82 |
| Berlin-CAT | 20051001 | 20051031 | 190 | 41.42 | 46.26 | 46.08 | 44.40 | 46.05 |
| Berlin-CAT | 20060401 | 20060430 | 231 | 7.61 | 68.55 | 69.62 | 72.43 | 8.71 |
| Berlin-CAT | 20060501 | 20060531 | 228 | 18.71 | 109.26 | 109.94 | 110.39 | 15.70 |
| Berlin-CAT | 20060601 | 20060630 | 226 | 43.53 | 62.51 | 61.49 | 62.92 | 41.41 |
| Berlin-CAT | 20060701 | 20060731 | 164 | 200.68 | 124.11 | 125.05 | 123.19 | 231.70 |
| Berlin-CAT | 20060801 | 20060831 | 219 | 28.98 | 96.94 | 96.35 | 97.93 | 61.88 |
| Berlin-CAT | 20060901 | 20060930 | 227 | 83.28 | 31.57 | 32.41 | 31.93 | 109.35 |
| Berlin-CAT | 20061001 | 20061031 | 220 | 75.73 | 32.02 | 31.85 | 31.51 | 79.28 |
| Berlin-CAT | 20070401 | 20070430 | 230 | 74.84 | 70.09 | 70.09 | 70.73 | 74.70 |
| Berlin-CAT | 20070501 | 20070531 | 38 | 65.78 | 70.27 | 70.15 | 70.01 | 59.57 |
| Berlin-CAT | 20070601 | 20070630 | 58 | 41.92 | 91.97 | 91.43 | 91.33 | 44.61 |
| Berlin-CAT | 20070701 | 20070731 | 79 | 25.02 | 54.80 | 52.69 | 52.53 | 33.07 |
| Berlin-CAT | 20070801 | 20070831 | 79 | 43.94 | 87.98 | 88.40 | 96.64 | 29.38 |
| Berlin-CAT | 20070901 | 20070930 | 79 | 61.38 | 55.74 | 57.59 | 59.36 | 60.93 |
| Tokyo-AAT | 20080501 | 20080531 | 25 | 514.71 | 276.57 | 276.61 | 254.88 | 548.00 |
| Tokyo-AAT | 20080601 | 20080630 | 46 | 623.82 | 415.89 | 415.94 | 480.31 | 638.11 |
| Tokyo-AAT | 20080701 | 20080731 | 67 | 724.84 | 223.93 | 223.95 | 226.28 | 830.93 |
| Tokyo-AAT | 20080801 | 20080831 | 89 | 699.42 | 284.87 | 284.84 | 292.10 | 844.41 |
| Tokyo-AAT | 20080901 | 20080930 | 110 | 603.28 | 248.31 | 248.28 | 230.61 | 683.63 |
| Tokyo-AAT | 20081001 | 20081030 | 5 | 508.26 | 0.00 | 0.00 | 0.00 | 585.64 |
| Tokyo-AAT | 20090301 | 20090331 | 35 | 331.67 | 99.61 | 99.62 | 84.19 | 145.00 |
| Tokyo-AAT | 20090401 | 20090430 | 37 | 302.85 | 52.61 | 52.62 | 42.25 | 110.11 |
| Tokyo-AAT | 20090501 | 20090531 | 37 | 167.30 | 23.19 | 23.19 | 21.03 | 57.83 |
| Tokyo-AAT | 20090601 | 20090630 | 37 | 184.98 | 33.90 | 33.90 | 36.25 | 135.19 |
| Tokyo-AAT | 20090701 | 20090731 | 37 | 121.99 | 104.18 | 104.18 | 105.18 | 41.84 |
| Tokyo-AAT | 20090801 | 20090831 | 19 | 55.41 | 57.10 | 57.10 | 57.10 | 136.61 |

Table 8: Root Mean Squared Error (RMSE) between the CME and the estimated weather futures $\hat{F}_{t,\tau_1,\tau_2,\lambda,\theta}$ under different localisation schemes ($\hat{\theta}$ under SeMe Locave, SeMe Locsep, SeMe Locmax)

# SFB 649 Discussion Paper Series 2011

For a complete list of Discussion Papers published by the SFB 649, please visit http://sfb649.wiwi.hu-berlin.de.

001 "Localising temperature risk" by Wolfgang Karl Härdle, Brenda López Cabrera, Ostap Okhrin and Weining Wang, January 2011.

**SFB 649, Ziegelstraße 13a, D-10117 Berlin**
**http://sfb649.wiwi.hu-berlin.de**

This research was supported by the Deutsche Forschungsgemeinschaft through the SFB 649 "Economic Risk".